To the Graduate Council:

I am submitting herewith a thesis written by Luis A. Bryan Y. entitled "Development and Experimental Evaluation of an Analytical Model of the Electronic Signal Processor for the Impedance Probe Used in the Advance Instrumentation for Reflood Studies (AIRS) Program." I recommend that it be accepted in partial fulfillment of the requirements for the degree of Master of Engineering, with a major in Electrical Engineering.

T. V. Blalock

T. V. Blalock, Major Professor

We have read this thesis and recommend its acceptance:

M. J. Roberts

T. F. Pawlicki

R. W. Rochelle

R. E. Bodenheimer

Accepted for the Council:

L. Evans Roth

Vice Chancellor
Graduate Studies and Research

DEVELOPMENT AND EXPERIMENTAL EVALUATION OF AN ANALYTICAL MODEL OF THE ELECTRONIC SIGNAL PROCESSOR FOR THE IMPEDANCE PROBE USED IN THE ADVANCE INSTRUMENTATION FOR REFLOOD STUDIES (AIRS) PROGRAM

A Thesis

Presented for the

Master of Engineering

Degree

The University of Tennessee, Knoxville

Luis A. Bryan Y.

December 1979

This thesis is dedicated

to my parents

Mr. Federico Bryan and

Mrs. Julieta Y. de Bryan

for their continuing love,

support, and encouragement

throughout my education.

ACKNOWLEDGMENTS

Any major work is brought to fruition through the efforts of many people. The author is very grateful for the invaluable guidance, patient, and helpful advice of Dr. T. V. Blalock, committee chairman, and Dr. T. J. Paulus. Appreciation is also extended to the committee members Dr. R. E. Bodenheimer, Dr. R. Rochelle, and Dr. M. J. Roberts.

Recognition is also expressed to the staff of R & D Electronics of E. G. & G. ORTEC for their help when needed, and to the members of E. G. & G. Oak Ridge Operations specially Charles Britton and Gregory Williams for their suggestions.

Last but certainly not least, the author conveys his deepest appreciation to Eric A. Bryan for his help with the art work and to Maria Coco Anderson and Marta Charris for their help with the first draft.

ABSTRACT

This investigation involves the development and analysis of a model of an electronic signal processor used in the Advance Instrumentation for Reflood Studies Program. The electronic circuit is based on a concept of Dr. M. J. Roberts at the Oak Ridge National Laboratory.

The purpose of the signal processor is to measure the impedance and changes in impedance of a two-phase flow inside a reactor during a reflood process. This measurement provides information about the velocity and void fraction of the flow. However, an exact analysis of the system, based on feedback theory, can be difficult, since the transfer function that expresses the system response is dependent on an impedance measurement taken in the feedback path of the signal processor.

This thesis presents a model which approximates very closely the actual electronic system. The model is based on a voltage-to-voltage transfer function approximation which is analysed using standard feedback system analysis.

Experimental results confirm the validity of the model developed and are also presented in this thesis.

TABLE OF CONTENTS

LIST OF TABLES

LIST OF FIGURES

FIGURE PAGE

CHAPTER 1

INTRODUCTION

The objective of this thesis is to develop and analyze a model of an electronic system that measures two-phase flow parameters. The development work was conducted under the Advance Instrumentation for Reflood Studies (AIRS) program at Oak Ridge National Laboratory (ORNL). The AIRS Electronic System was developed by E. G. & G. Oak Ridge Operations under contract 62X-45745V to the Nuclear Division of Union Carbide Corporation.

The function of the AIRS Electronic System is to measure three-dimensional two-phase flow parameters in the upper plenum and core of two German and two Japanese pressurized-water reactor loss-of-coolant accident in nonnuclear reflood test facilities. AIRS is part of the national program on water reactor safety sponsored by the United States Nuclear Regulatory Commission, and is also part of the joint 3-D program on reflood studies involving Japan, West Germany, and the United States [1].

1.1. Scope of Work

This thesis will present a development of a model which approximates very closely the AIRS Electronic System. The work presented here will be organized as follows:

Chapter 2 covers the method used to measure the two-phase flow inside the reactor when a loss-of-coolant accident occurs, and some previous experimental work.

Chapter 3 deals with the analysis of the AIRS Electronic System. In this chapter, a description of the Roberts loop is made. Oscillation stability analysis and closed-loop frequency response are studied based on the model developed.

Chapter 4 presents the system performance and the scheme used to measure the transient response of the system. This test was performed with both the actual system and the model developed.

Chapter 5 describes the important points that must be considered when optimizing the system.

Chapter 6 states some conclusions and suggestions for further work.

CHAPTER 2

BACKGROUND

2.1. Measurement of Two-Phase Flow

Measurement of two-phase flow starts when a loss-of-coolant accident occurs, and the emergency coolant begins to reflood the fuel elements inside the reactor. This reflood phase begins to cool the fuel rods, which are at extremely high temperatures. During this quenching, the flow appears in two phases, steam and water. To study this reflood process, the void fraction (ratio of volume of steam to the total volume), and the velocity of the flow must be known. Analysis predicts that this two-phase flow condition generates a change in the impedance of the fluid inside the reactor, thus, leading to the conclusion that a method to detect the impedance and change in impedance was needed. A method was developed at ORNL to detect these impedance changes involving the insertion of a probe into the flow. This probe has been found to have an impedance consisting of a capacitance in parallel with a resistor; therefore, the probe impedance may be represented as

$$Z_{probe} = R \parallel \frac{1}{j\omega c} = \frac{1}{\frac{1}{R} + j\omega c} \quad . \tag{2.1}$$

However, the probe is basically capacitive, and the resistive component is mainly due to the impurities contained in the water used for the reflood process. Analysis determined that values of probe capacitance could change over an 80 to 1 dynamic range since the dielectric constant of water is about 80, thus creating different impedance measurements for the steam to water variations [2]. Consequently, analysis was made, and it was found that at small void fractions, the conductance $(\frac{1}{R})$ varies according to changes in the void fraction; however, at high void fraction with no water bridging, there is a small amount of water and the changes in conductance are negligible, then Eq. (2.1) can be approximated by

$$|Z|_{probe} = |\frac{1}{j\omega C}| \quad . \tag{2.2}$$

Here small changes in the capacitive part of the impedance occur when water or steam passes through the electrodes of the probes, and correlation between two sensors can be used to infer information about the velocity and direction of the flow [2].

The probes developed at ORNL can take many configurations. Some small probes called "prong probes," and "flag probes," are characterized by all-air capacitance values of 0.1 to 1.0 pF. Another type, somewhat larger, are called "string probes," and have all-air capacitance values from 2.0 to 12.0 pF [1]. These different configurations are shown in Fig. 2.1.

Problems were encountered in the fabrication of these probes due to the thermal stress they must withstand (600° to 900° Celsius) at quench in a very short period of time, thus implying that special materials were needed (ceramic coated) to operate at these sudden changes in temperature. Due to the high temperatures, the electronic signal processor is at a remote location so that interconnections between the

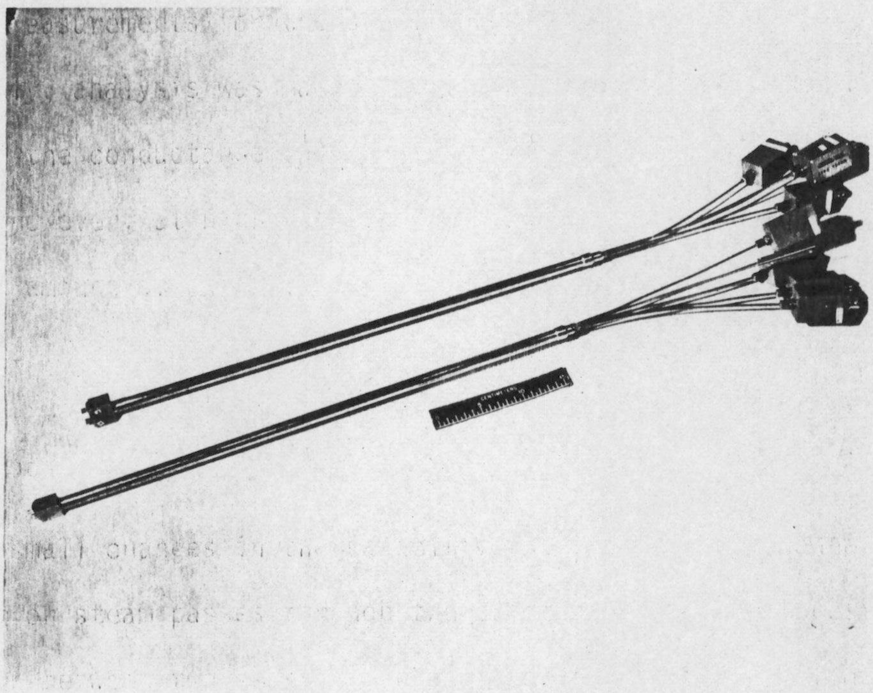

(a) Prong and flag probe

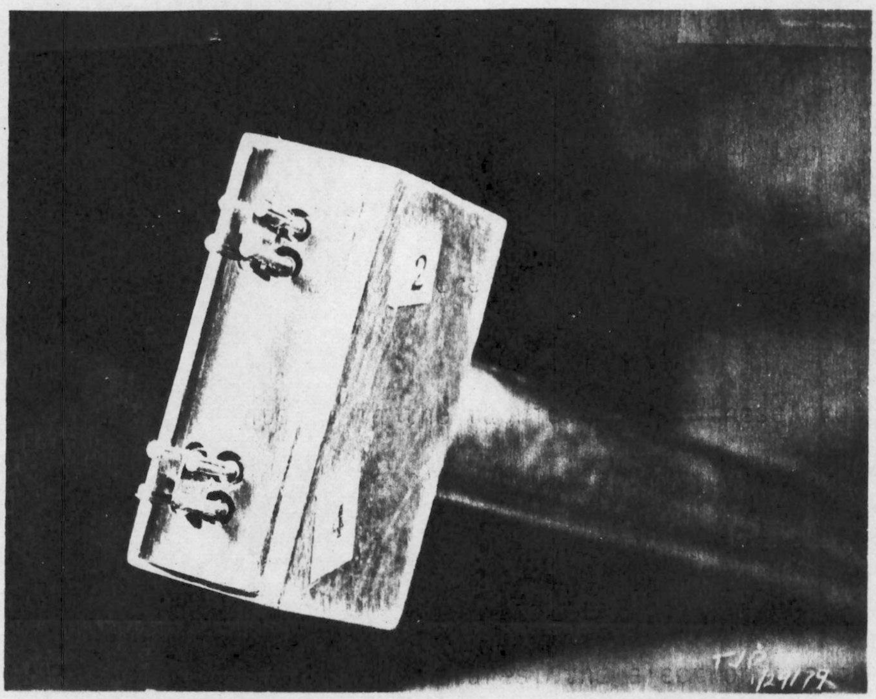

(b) Flag probe

Figure 2.1. Different probe configurations

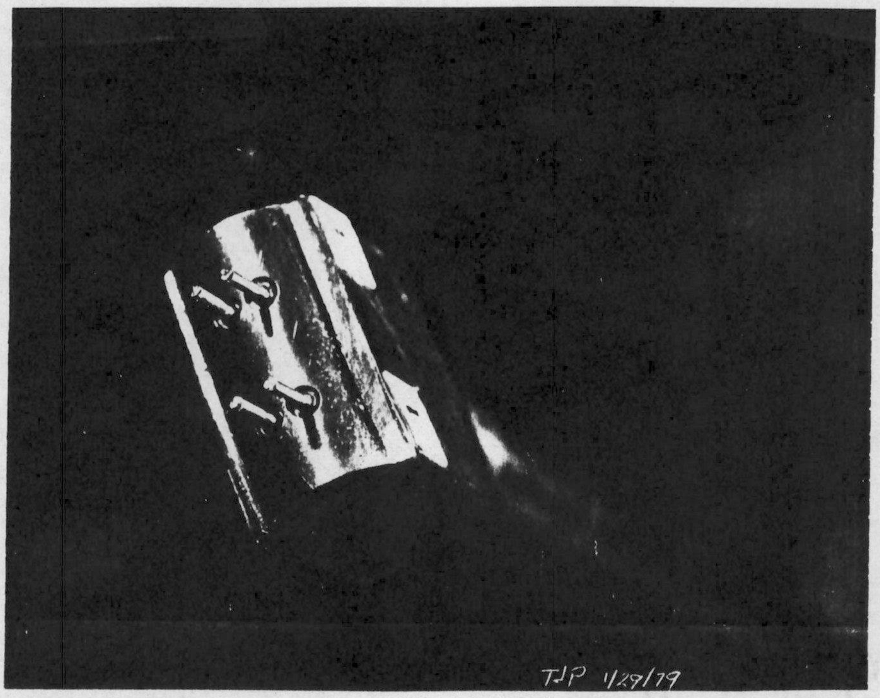

(c) Prong probe

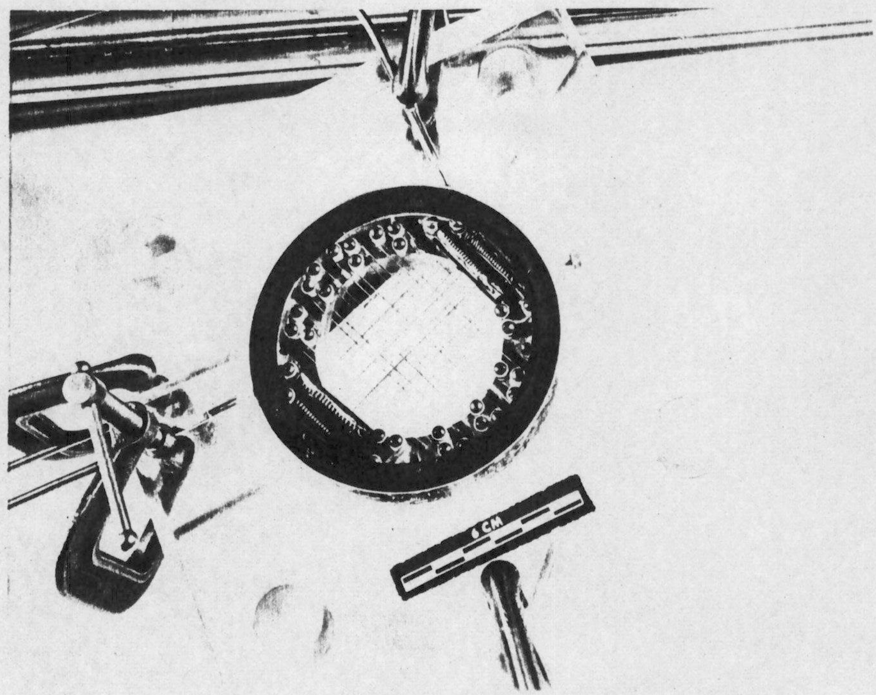

(d) String probe

Figure 2.1. (continued)

system and the probe were needed. To reduce electromagnetic interference, special triaxial cable was used.

2.2. Previous Experimental Work

Early studies were conducted by Roberts and others at ORNL in laboratory experiments using the air-water and steam-water loop facilities, where impedance changes in the two-phase flow were simulated and measured.

The work presented here was directed by Dr. T. J. Paulus of E. G. & G. Oak Ridge Operations and is a continuation and further development of the earlier work at ORNL. All the experiments presented in this thesis used a capacitor to simulate the probe capacitance and changes in probe capacitance in the two-phase flow.

CHAPTER 3

FREQUENCY RESPONSE ANALYSIS OF AIRS ELECTRONIC SIGNAL PROCESSOR

3.1. Introduction

The operation of the Roberts loop will be described in this chapter, and the dependent current source approximation ($Ke^{-S\tau}$) used to develop the electronic model will be discussed. Oscillation stability analysis and calculated and experimental closed-loop response are also presented based on the model developed.

3.2. Description of the Roberts Loop

The principle of the Roberts loop is to produce an analog output voltage proportional to the magnitude of the impedance of the probe in the two-phase flow. The complete schematic of the electronic loop and phase detection circuit is shown in Fig. 3.1.

The Roberts loop can be interpreted as a circuit that is capable of indicating an impedance change by incrementing an output voltage. In simple terms, the Roberts loop can be interpreted as an integrator with two major feedback loops. One defined by the probe circuit and the other by the integrator's network. This interpretation is shown in a functional diagram in Fig. 3.2. The input signal to the integrator is a fixed dc voltage (V_{set}). The output voltage of the integrator (V_{out}) depends on both, the dc input voltage and the equivalent feedback impedance of the integrator. This feedback impedance changes as probe

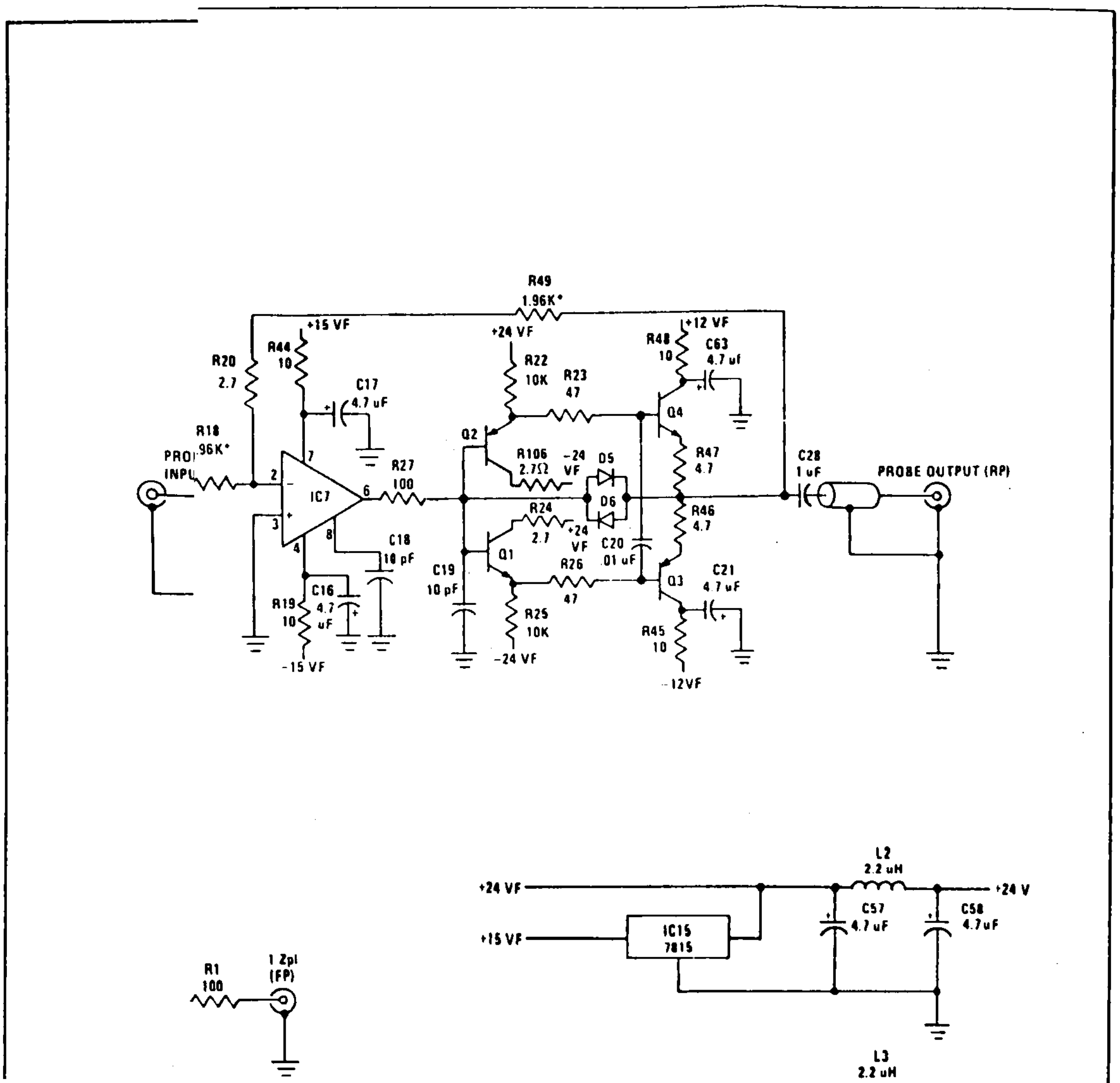

Figure 3.1. Complete schematic of electronic loop and phase detection circuit

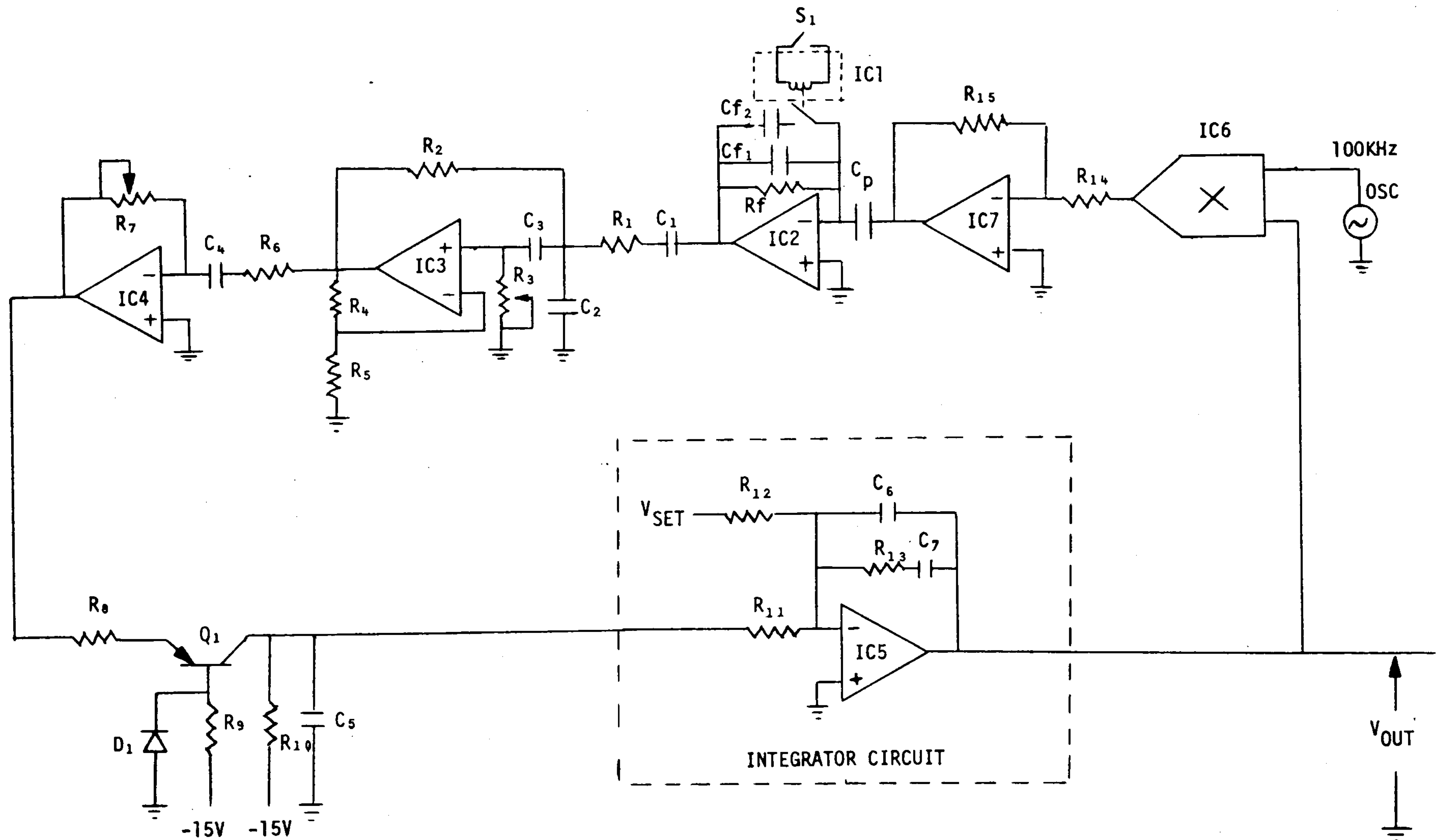

Figure 3.2. Functional diagram of the Roberts loop

(C_p) variations occur causing a change in the output voltage of the integrator circuit.

Referring to Fig. 3.2, the integrator Op Amp is IC5 and its integrating circuit is composed of C6 (integrator capacitor) and R13 and C7 (compensating and shaping network). Resistor R13 and capacitor C7 are chosen to shape the transient response of the system.

The probe is coupled to the integrator circuit using a signal derived from the 100 KHz sine wave reference signal, requiring both modulation and demodulation. The output of the integrator modulates the 100 KHz sine wave in the multiplier circuit (IC6). The output of the multiplier is connected to a driver stage (IC7) whose voltage gain is unity set by R15/R14. Thus the signal fed to the probe is a 100 KHz sine wave whose amplitude is proportional to the voltage at the output of the integrator.

The probe couples the 100 KHz signal into the input of a charge sensitive preamplifier (IC2) which detects the ratio of probe capacitance to a reference capacitance. The feedback components of IC2 are R_{f1} which provides a dc path, and the reference capacitors C_{f1} and C_{f2} which set the voltage gain. A switch controls the relay IC1 which switches C_{f2} for large values of probe capacitance. The value of C_{f1} and C_{f2} will be referred to as C_f in the succeeding chapters. The voltage gain of IC2 will be dependent on the value of probe capacitance (C_p) and C_f, being approximately C_p/C_f.

The IC3 circuit is a bandpass filter which helps reject any low frequency signal from power lines. The AC coupling furnished by C1 and C4 provides additional low frequency rejection.

A variable gain stage (IC4 circuit) follows the bandpass filter. The voltage gain of this circuit can be varied by adjusting R7.

Following the gain stage, a half-wave rectifier is present (Q1). Resistor R8 sets the amount of current into the emitter of Q1. Under normal operation, the output voltage of IC4 is at 2 volts peak sine wave (modulated signal). The function of D1 is to compensate the transistor voltage drop of 0.6 volts. The output of the half-wave rectifier is filtered by C5 and is also fed to the integrator circuit (IC5) through R11.

The probe circuit is composed of the modulator (multiplier) and demodulator (rectifier) sections, and consists of: the multiplier, input stage, bandpass filter, a variable gain stage, and a rectifier. The voltage levels from the output of the preamplifier to the input of the rectifier are held at constant amplitude. This is explained in the following matter: assume that during normal operation the output of the integrator is 10 volts signal for a minimum value of probe capacitance (C_{pmin}); then, an increase in probe capacitance will cause a decrease in the output voltage of the rectifier and the loop will correct the output of the integrator to keep the constant amplitude mentioned previously. The output voltage of the integrator is inversely proportional to the value of probe capacitance in the two-phase flow.

Section 3.3 will explain in more detail how an approximation is made, which will lead to the model development. This approximation is valid when the modulating signal is much slower than the carrier signal.

3.3. The K $e^{-S\tau}$ Approximation

In the preceding section it was noted that the output voltage of the integrator acts as the modulating signal of the system, which is inversely proportional to a probe capacitance change in the two-phase flow. These probe capacitance changes have been expected to occur at a maximum frequency of 1KHz [3]; which means that a maximum modulating frequency would be about 1KHz.

Previous analysis done by Dr. T. V. Blalock [4], at The University of Tennessee, show that the modulation-demodulation section can be approximated by a constant K times a delay in time τ_d defined by

$$\tau_d = \frac{\theta_c}{2\pi f_c} \quad . \tag{3.1}$$

This same time delay must exist also for the low frequency modulation signal which flows around the entire loop. Therefore, for the "loop signal"

$$\tau_d = \frac{\theta_m}{2\pi T_{loop}} = \frac{\theta_c}{2\pi f_c} \quad , \tag{3.2}$$

thus

$$\theta_m = \frac{f}{f_c}\,\theta_c \quad ,$$

where fc is the carrier frequency, and θ_m is the total phase shift of the modulation-demodulation section at the modulation frequency f if the modulation frequency is much slower than the carrier frequency. The constant K times a delay τ can be expressed in Laplace form as

$$Ke^{-s\tau} \quad .$$

The modulation-demodulation section is composed of the probe circuit as mentioned in the previous section. If the sum of the phase shifts in the probe circuit at the carrier frequency is small, the delay τ will be also very small, thus the modulation-demodulation section can be approximated only by the constant K. To find the amount of phase shift in the modulation-demodulation section, it is necessary to investigate the frequency response of each of the stages that constitute the probe circuit. This investigation follows.

Amplitude modulation is accomplished with an analog multiplier. This multiplier has two inputs, one provided by an oscillator which generates a 10 volt peak sine wave at a frequency of 100 KHz, and the other is the output voltage of the integrator. The first one is the carrier wave and the second one is the modulating wave. The input to the multiplier from the oscillator can be expressed as [5]

$$E_c = E_{cp} \sin 2\pi f_c t \tag{3.3}$$

where E_{cp} is the peak value of the carrier wave and f_c is the carrier frequency. The modulating signal is described by

$$E_m = V_o[1 + \sin 2\pi f_m t] \tag{3.4}$$

where V_o is the peak modulating signal and f_m is the modulating frequency. The output of the multiplier is defined by

$$V_{o(mult)} = \frac{E_m\ E_c}{c}$$

$$= V_o E_{cp} \sin 2\pi f_c\ t + V_o E_{cp} (\sin 2\pi f_c t)(\sin 2\pi f_m t) \qquad (3.5)$$

where c is a constant equal to 10 for this multiplier. Equation (3.4) can also be expressed using trigonometric identities as

$$V_{o(mult)} = \frac{V_o E_{cp}}{2o} \sin 2\pi f_c t$$

$$+ \frac{V_o E_{cp}}{2} \cos 2\pi (f_c - f_m) t - \frac{V_o E_{cp}}{2} \cos 2\pi (f_c + f_m) t \quad . \qquad (3.6)$$

From Eq. (3.5), it can be seen that V_o is composed of two sine waves with frequencies different from either E_c or E_m. They are the sum frequency $f_c + f_m$, and the difference frequency $f_c - f_m$. Note that the carrier is also present. These resulting frequencies are called upper and lower side frequencies. Figure 3.3 shows a block diagram of the multiplier and its frequency spectrum.

One input to the multiplier is held constant, the carrier signal (oscillator), while the other is varied at the modulating frequency (C_p change). A typical first order response for this case, will have 45° phase lag at the -3db frequency, f_o, of the multiplier. For this multiplier, the -3db frequency is 100 KHz. Wait et al, show that at frequencies well below f_o, the phase shift can be estimated as [6]

$$\theta_{mult} = -\frac{f}{f_o} \text{ rad} \quad \text{for } f \ll f_o \quad , \qquad (3.7)$$

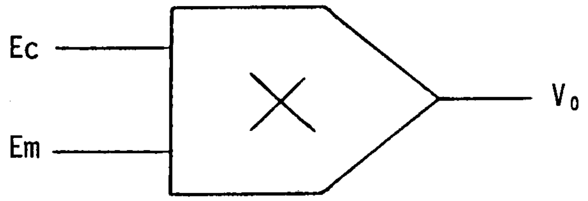

(a)

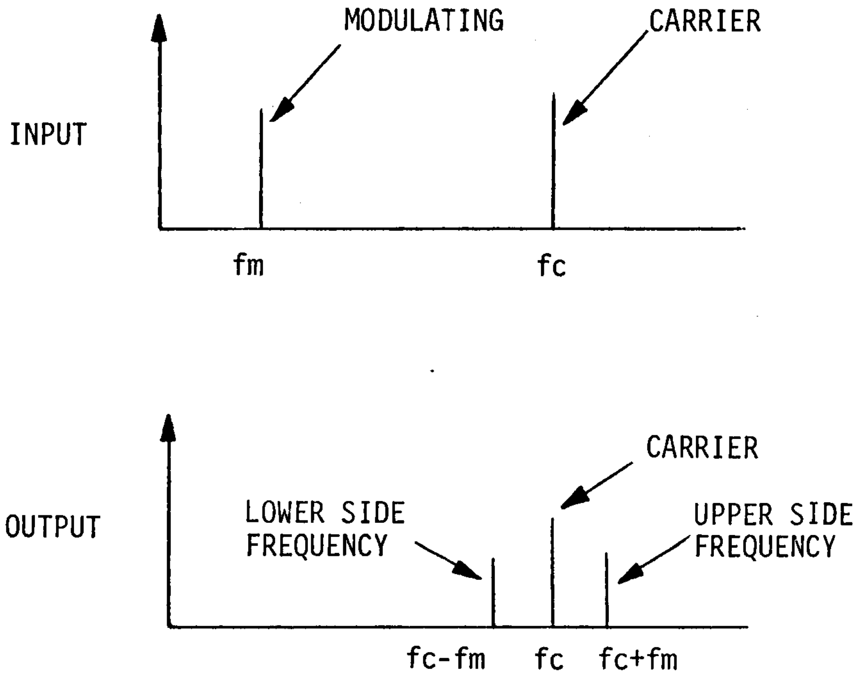

(b)

Figure 3.3. Multiplier block diagram (a) and frequency spectrum (b)

where fo is the -3db frequency, and f is the modulating frequency. Equation (3.7) implies that the phase shift of the multiplier is negligible when the modulating signal is much slower than the carrier signal.

The output of the multiplier (AM signal) is followed by a driver stage which is composed of an operational amplifier driving a diamond driver power amplifier. The gain of this stage is unity, and the frequency response is well beyond 100 KHz. The amount of phase shift of this driver stage is also negligible. This stage drives the signal to the probe location.

The preamplifier section (input stage), that follows, has an output signal proportional to the capacitance ratio of the probe to a reference capacitance. The Laplace transfer function of the preamplifier is defined by

$$H_1 = \frac{V_2}{V_1} = \frac{SRC_p}{SRC_f+1} = \frac{Cp}{Cf}\ \frac{S}{S+\frac{1}{RC_f}} \quad . \tag{3.8}$$

Figure 3.4 shows a simplified schematic of the preamplifier section and the Bode plot.

A bandpass Sallen-Key active filter follows the input stage. Figure 3.5 shows a simplified circuit diagram of this filter. The Laplace transfer function of the active filter is defined by [6]

$$H_{(S)BPF} = \frac{S\,\frac{K_0}{R_1C_1}}{S^2 + S\left[\frac{1}{R_1C_1} + \frac{1}{R_3C_1} + \frac{1}{R_3C_2} + \frac{(1-K_0)}{R_2C_1}\right] + \left[\frac{\frac{1}{R_1} + \frac{1}{R_2}}{R_3C_1C_2}\right]} \tag{3.9}$$

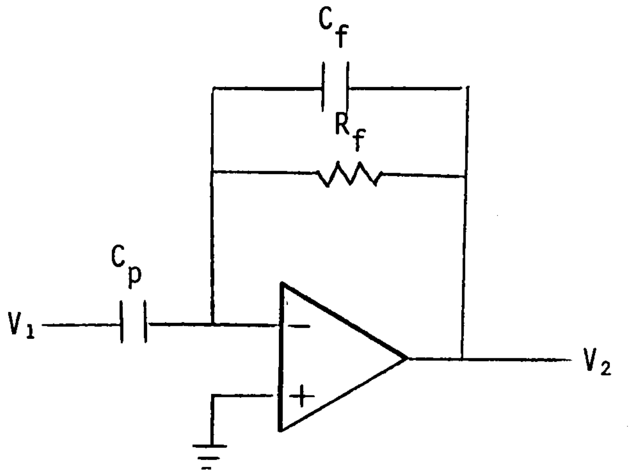

(a)

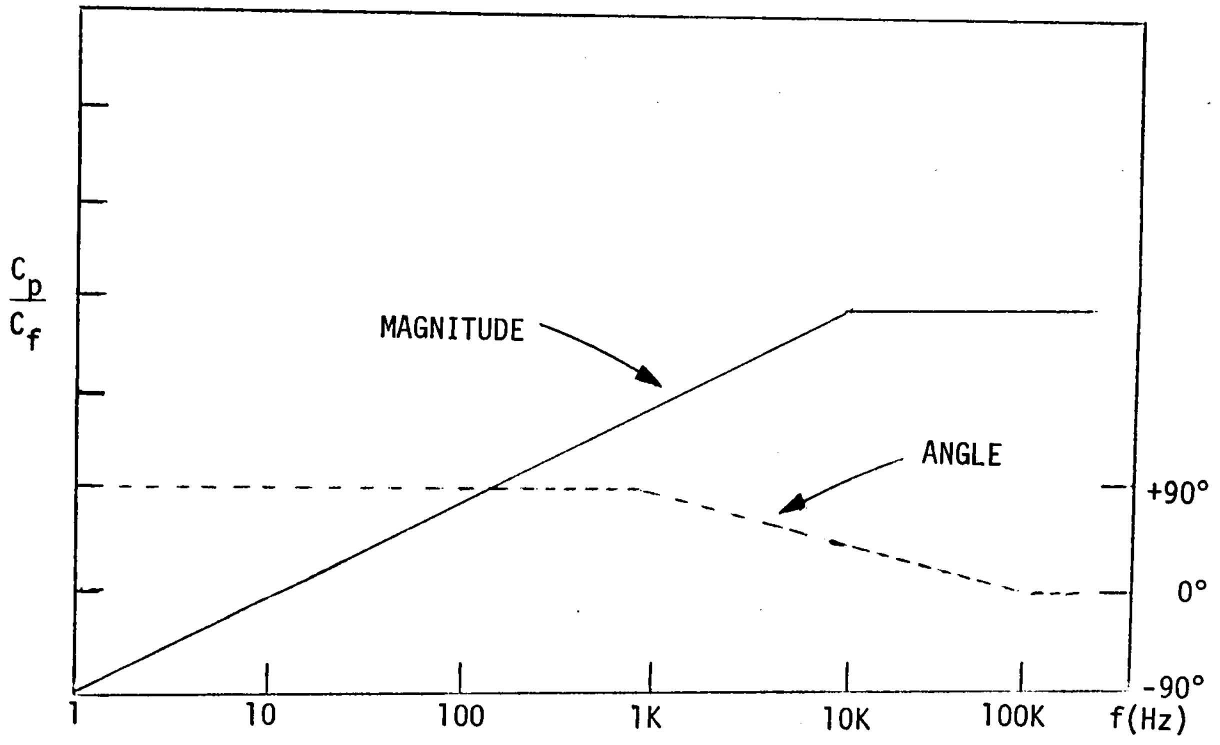

(b)

Figure 3.4. Schematic of preamplifier section (a) and Bode plot (b)

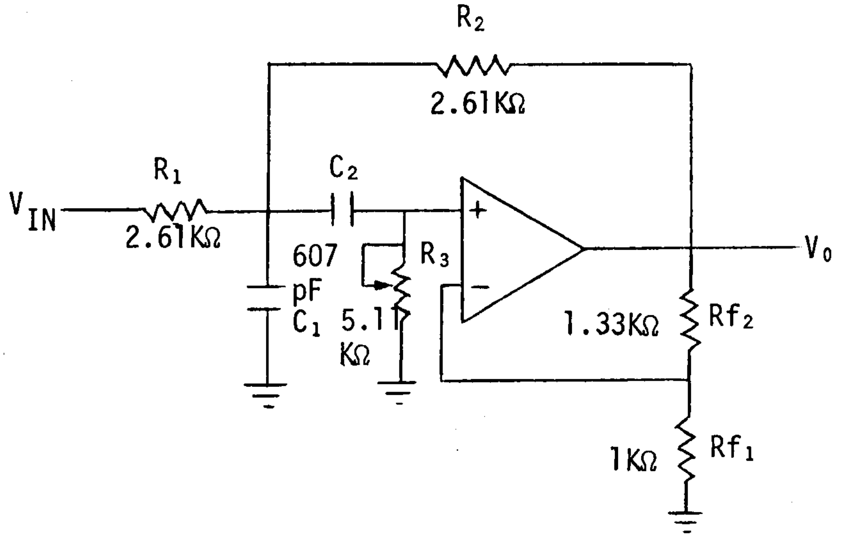

(a)

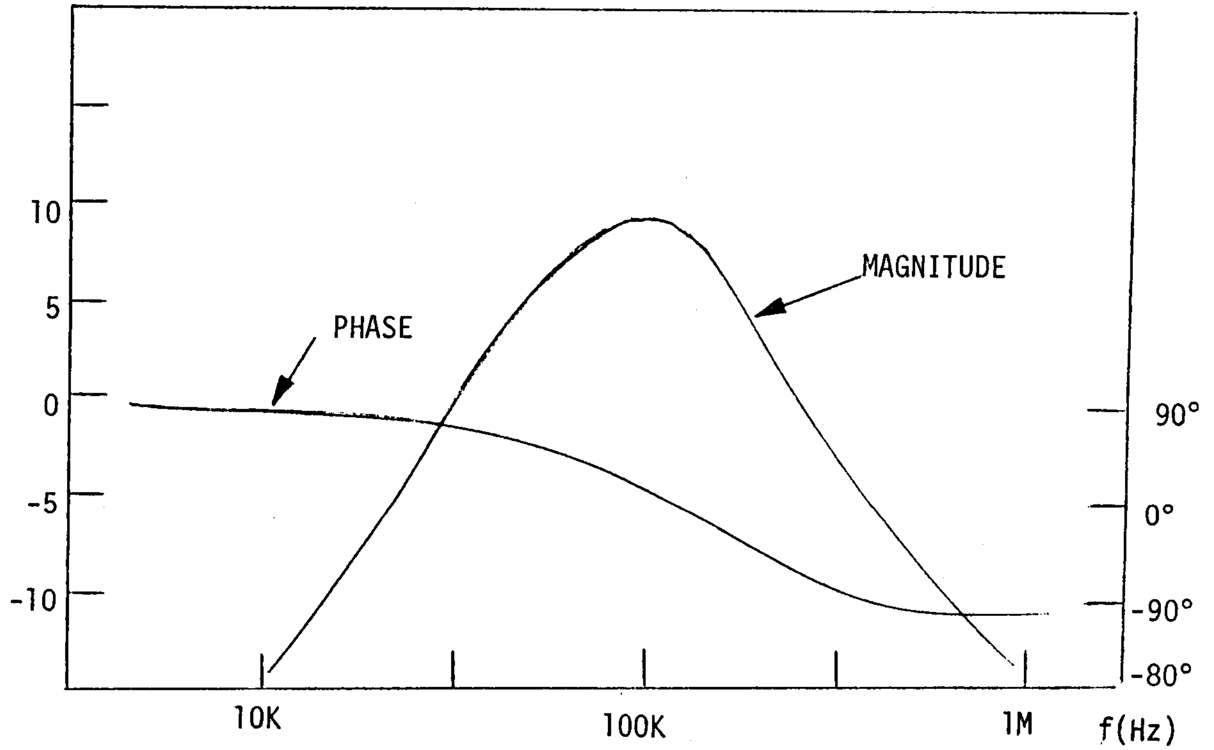

(b)

Figure 3.5. Bandpass filter circuit (a) and frequency response (b)

or in a simplified form

$$H_{(s)_{BPF}} = \frac{Hs}{s^2 + sa_1 + a_0} \quad . \tag{3.10}$$

The resonant frequency ω_0 is

$$\omega_0 = \sqrt{\frac{a_0}{a_1}} \quad \text{rad/sec} \quad , \tag{3.11}$$

and the Bandwidth (BW)

$$BW = a_1 \quad . \tag{3.12}$$

The Q factor is

$$Q = \frac{\sqrt{a_0}}{a_1} = \frac{\omega_0}{BW} \quad , \tag{3.13}$$

and the gain at resonance H_0 is expressed as

$$H_0 = \frac{K_0}{3-K_0} \quad , \tag{3.14}$$

where K_0 is the d.c. gain

$$K_0 = \frac{Rf_2}{Rf_1} + 1 \quad . \tag{3.15}$$

Therefore, the characteristics of the bandpass filter (substituting the component values) are

$$H_{(s)_{BPF}} = \frac{S(1451772.74)}{S^2 + S(436495.53) + (4.0699 \times 10^{11})} \quad , \tag{3.16}$$

where

$$\omega_0 \simeq 100 \text{ KHz} \quad , \tag{3.17}$$

$$BW \approx 70 \text{ KHz} \quad , \tag{3.18}$$

$$Q \approx 1.43 \quad , \tag{3.19}$$

$$K_0 \approx 2.3 \quad , \tag{3.20}$$

$$H_0 \approx 3.3 \quad . \tag{3.21}$$

The frequency response of the filter is also shown in Fig. 3.5. At the 100 KHz carrier frequency the gain is approximately 3.3 with a phase shift of about 4 degrees. However, the phase shift of the filter is adjusted to 0° by R3.

A variable gain stage follows the filter, Fig. 3.6 shows a simple schematic of the variable gain stage. The gain stage provides a constant output voltage of approximately 2 volts peak to the input of the rectifier (demodulating) section when the loop is in normal operation. The gain (Ag) of this stage is defined by

$$Ag = \frac{Vout}{Vin} = \frac{-R_f}{R_1} \tag{3.22}$$

where R_f is the total feedback resistance selected. The frequency response of this gain stage is well beyond 100 KHz with a negligible phase shift at 100 KHz.

This gain section is followed by the demodulation stage. Demodulation is performed by an envelope detector [7]. This detector uses a half wave rectifier. The equivalent circuit is shown in Fig. 3.7. The input peak voltage is held constant at about 2 volts. Therefore, the amount of current provided from the collector of Q1 is

$$I_m = \frac{Vin(peak)}{\pi \cdot 383} \approx 1.7 \text{ mA} \quad . \tag{3.23}$$

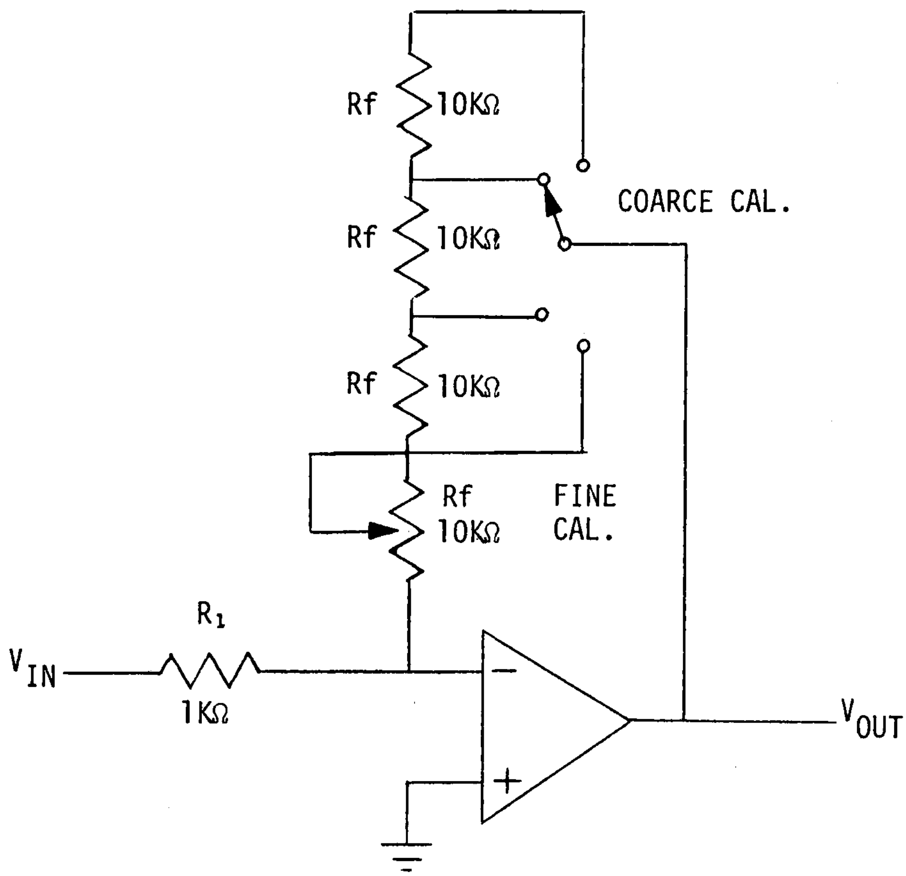

Figure 3.6. Variable gain stage

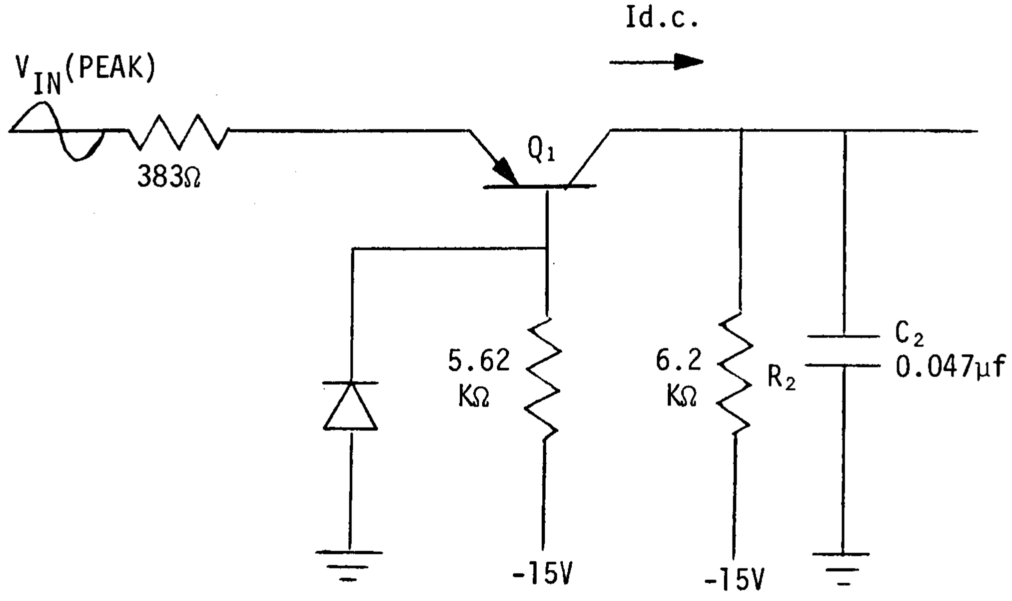

Figure 3.7. Equivalent circuit of rectifier-demodulation section

The rectified output voltage at the collector of Q1 is approximately -3.1 volts. The resistor R_2 and capacitor C_2 define the ripple voltage of the demodulated signal. The ripple factor is determined by [8]

$$RF = \omega R_2 C_2 = 2\pi f R_2 C_2 \quad . \tag{3.24}$$

A plot of ripple factor as a function of ωRC is shown in Fig. 3.8 [8].

The output of the rectifier is fed to the integrator circuit (shown in Fig. 3.9). The voltage at node V_1 is maintained at a virtual ground, therefore, R_3 can be neglected in the calculation of loop transmission. When there is a probe capacitance change, the output of the rectifier creates a fluctuation in current, which makes the voltage at the V_{in} node of the integrator be different from the d.c. set voltage (V_{set}), thus, creating the error signal that is integrated and proportional to the probe change. The Laplace transfer function of the integrator is

$$H_{(s)_{int}} = \frac{V_{out}}{V_{in}} = \frac{(1 + S\, R_2 C_2)}{R_1 (C_2 + C_1)\; s\left(1 + s\, \frac{R_2 C_2 C_1}{C_1 + C_2}\right)} \quad . \tag{3.25}$$

Equation (3.25) can also be expressed in terms of the -3db critical frequencies associated with each pole and zero in the s-plane (Laplace form). Substituting component values and expressing Eq. (3.25) in the frequency domain gives

$$H_{(jf)_{int}} = 9469.7 \; \frac{\left(1 + \frac{jf}{fz}\right)}{jf\left(1 + \frac{jf}{fp_1}\right)} \quad , \tag{3.26}$$

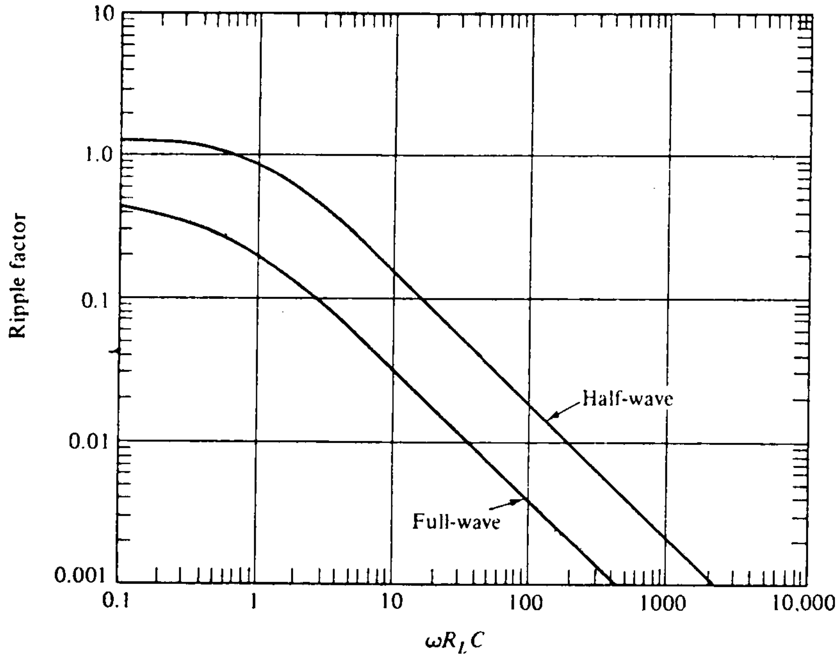

Figure 3.8. Ripple factor as a function of ωRC (from Pierce & Paulus)

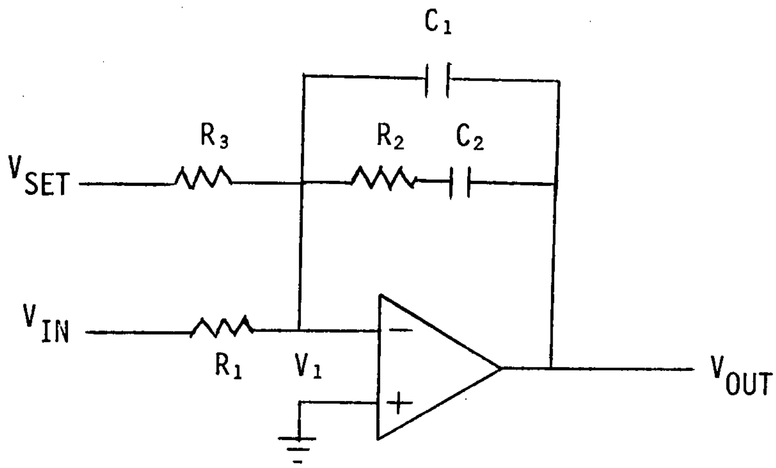

(a)

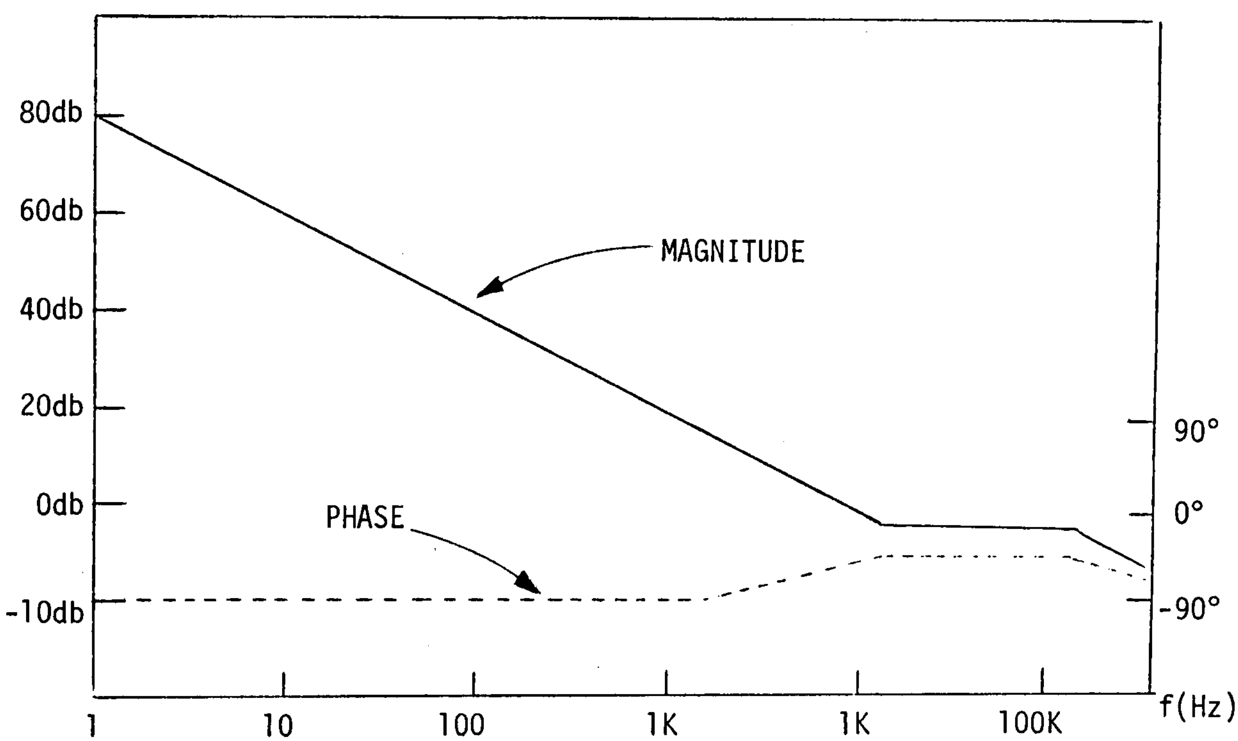

(b)

Figure 3.9. Integrator circuit (a) and Bode plot (b)

where

$$fz = \frac{1}{2\pi \cdot R_2 \cdot C_2} \simeq 13.1 \text{ KHz} \quad , \tag{3.27}$$

and

$$fp_1 = \frac{(C_1 + C_2)}{2\pi \cdot R_2 \cdot C_1 \cdot C_2} \simeq 247 \text{ KHz} \quad . \tag{3.28}$$

The Bode plot for the integrator circuit is also shown in Fig. 3.9.

It is interesting to note that the sum of the phase shift in the probe circuit is relatively small at the carrier frequency of 100 KHz. Neglecting the small delay in time τ, defined previously, the probe circuit can be represented by a dependent current source since the output current of the rectifier is dependent on the output voltage of the integrator (input to the multiplier) to drive the specific probe capacitance. Any change in the rectified voltage caused by a change in probe capacitance will inject more current, thus creating an error voltage signal at the input of the integrator.

Since the delay time is small, the dependent current source approximation (probe circuit) can be represented only by the constant K. Figure 3.10 shows the block diagram of the probe circuit as a dependent current source. Using this approximation (probe circuit as a dependent current source) the Roberts loop can be simplified by replacing the current source Fig. 3.10 in the schematic diagram interpretation of the loop shown in Fig. 3.2; this is shown in Fig. 3.11.

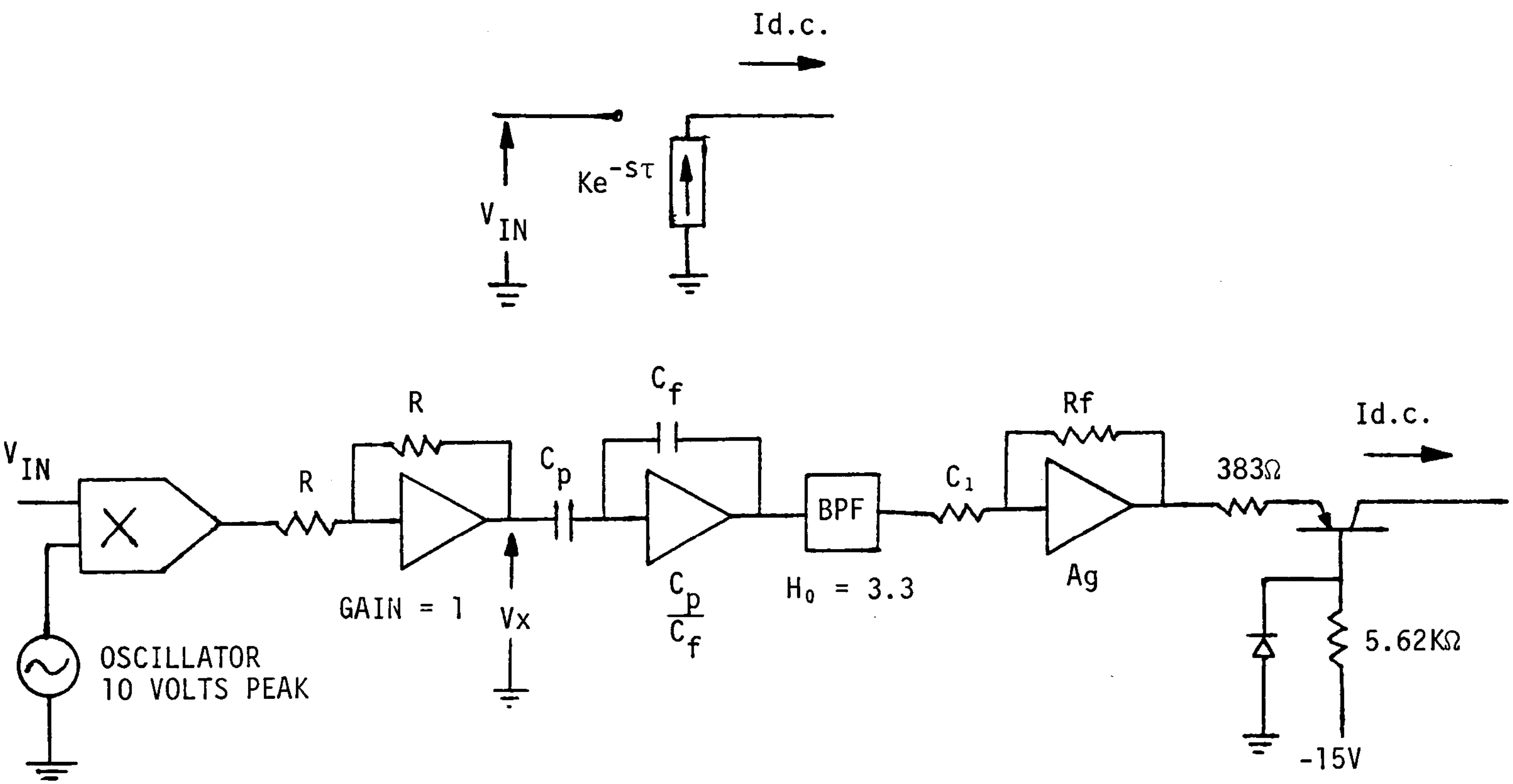

Figure 3.10. Block diagram of probe circuit as a dependent current source

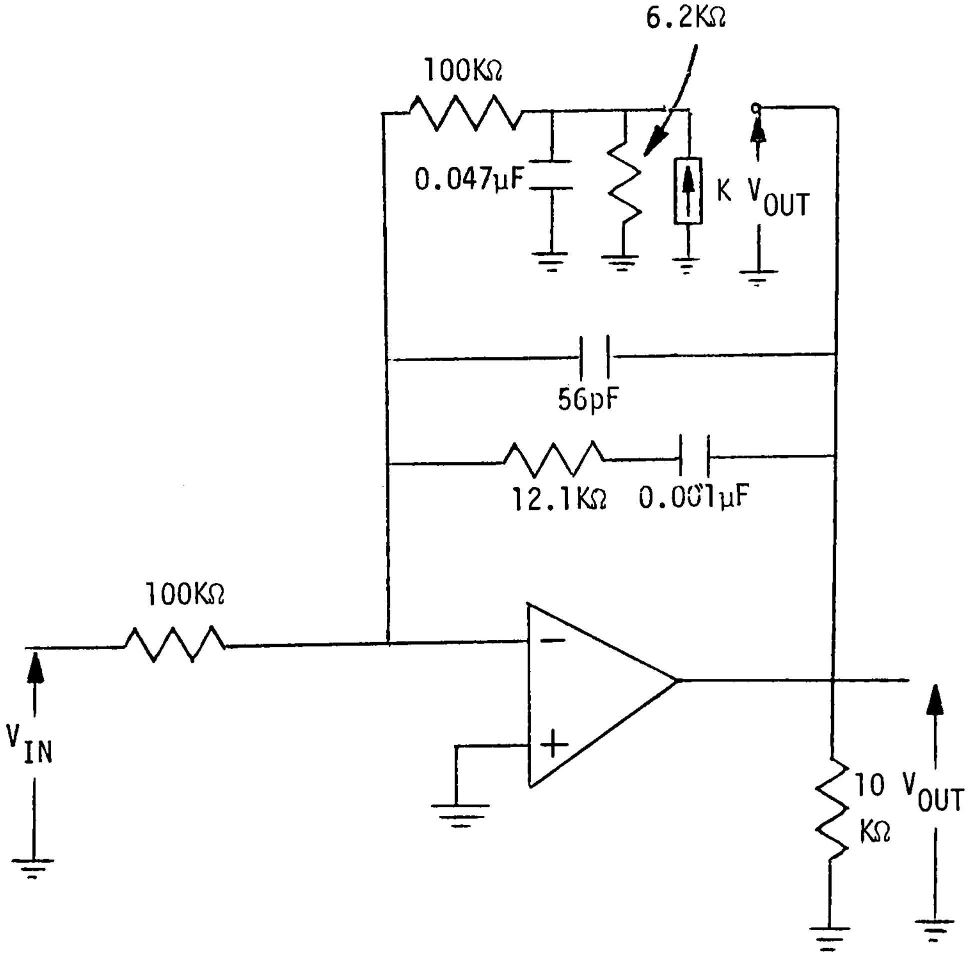

Figure 3.11. Interpretation of the Roberts loop with dependent current source

Figure 3.11 shows the model of the Roberts loop (based on the $K\ e^{-s\tau}$ approximation) which will be analyzed. The next section will show how the value of K is obtained for certain values of probe capacitance related to its corresponding output voltage.

3.4. Definition of "K" as a Dependent Current Source

The $K\ e^{-s\tau}$ approximation will permit, as mentioned before, and easier analysis of the Roberts loop. This section will show how the value of K is derived from the probe circuit. Referring to Fig. 3.10, K can be described by

$$K = \frac{Cp}{Cf} \cdot H_0 \cdot Ag \cdot \frac{1}{\pi \cdot 383} \quad , \tag{3.29}$$

where Cp is the probe capacitance, Cf the reference capacitance, H_0 the gain of the bandpass filter at resonance (100 KHz), Ag the gain of the variable stage, and $\frac{1}{\pi \cdot 383}$ is the gain of the rectifier. The π factor in the denominator is introduced due to the halfwave rectification of the sine wave (half a complete 2π cycle).

The value of Ag (variable gain) must be calculated to set the input voltage (peak) of the rectifier at a constant value. This input voltage defines the amount of current provided by the rectifier demodulation section, which sets a voltage level equal to the d.c. set voltage with opposite polarity.

Figure 3.12 shows the circuit diagram used to calculate Ag. The voltage at V_1 (Fig. 3.12) must be approximately -3V d.c., which will set the input of the integrator at zero volts d.c. allowing any error

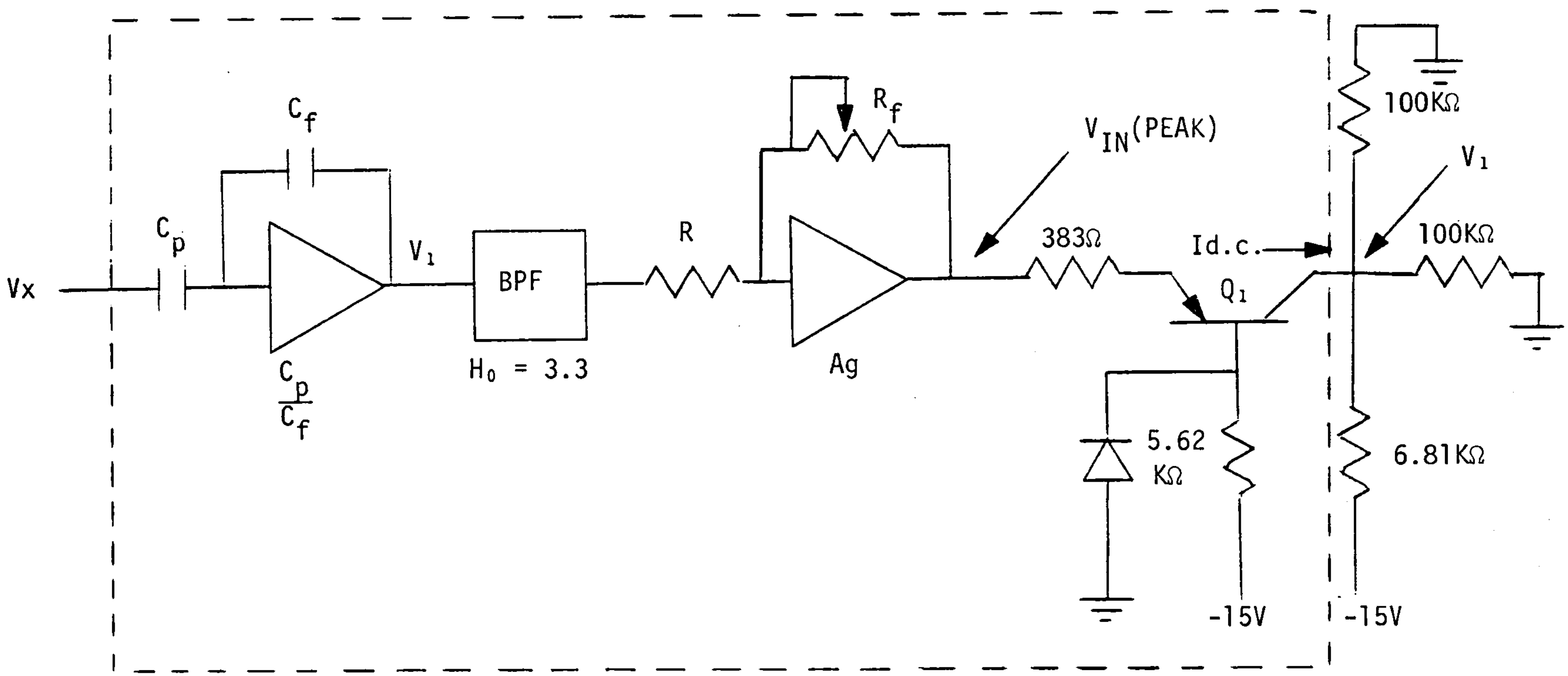

Figure 3.12. Circuit used to calculate Ag

signal to be created for a change in C_p. The current needed from the rectifier (I_m) can be calculated by simple circuit analysis:

$$I_m = \frac{12V}{6.8k} + \frac{-3V}{100k} + \frac{-3V}{100k} = 1.7 \text{ mA} \quad . \tag{3.30}$$

This current will set V_1 to approximately -3 Volts d.c. Therefore, the

$$\text{Vin (peak)} = I_m \times 383 \times \pi \simeq 2.048\text{V peak} \quad . \tag{3.31}$$

This input voltage (Vin(peak)) is also a function of Vx (refer to Fig. 3.10) which is the output voltage of the driver stage. Therefore, Vin (peak) can be expressed as

$$\text{Vin (peak)} = V_x \cdot \frac{C_p}{C_f} \cdot HO \cdot Ag \quad . \tag{3.32}$$

For the case of C_{pmin}, V_x is equal to 10 volts. Replacing the values known and solving for Ag we have

$$Ag = \frac{(2.048)\ C_f}{V_x \cdot C_p \cdot (3.3)} \quad . \tag{3.33}$$

Substituting values in Eq. (3.29) K is

$$K = C_p(1.702 \times 10^{-4}) \quad . \tag{3.34}$$

Equation (3.34) shows how the value of the dependent current source approximation is described. Note that Eq. (3.34) depends on the probe capacitance. This implies that for a particular value of C_p an output voltage can be set. The settings for V_{out} (or $|Z|$) are selected for the specific probe capacitance. If for a value of C_p, a 10 volt output is selected, then for 10 C_p the output would be 1 volt. Thus, the output voltage of the system is inversely proportional to the probe capacitance, because an increase in C_p will cause the value of K to increase which increases the voltage V_1 (Fig. 3.12). Since the loop will try to maintain a virtual ground at the integrator input, the output voltage of the integrator must decrease to keep the preamplifier stage output constant for the new C_p/C_f voltage gain. The output of the system can be set to 10 volts for any value of C_p, thus this C_p value becomes C_{pmin}, and for any increase by a factor of 10 in C_p the output voltage will decrease also by a factor of 10.

3.5. Oscillation Stability Analysis

A system is said to be stable against oscillation if a small impressed disturbance, which itself dies out, results in a response which dies out. A system is unstable if such disturbance results in a response which goes on indefinitely and increases until it is limited by a nonlinearity in the system [9]. Bode analysis is often used to study the magnitude and phase angle of the system. In this type of analysis, a negative feedback system will be stable if the phase angle does not exceed 180° when the magnitude is equal to or greater than unity. The phase margin, PM, is given by

$$PM = 180° - \underline{\angle T} \quad , \tag{3.35}$$

where $\underline{\angle T}$ is the angle at which the loop transmission magnitude ($|T|$) is unity [8].

To determine the loop transmission T, we need to break the closed-loop at a point without any change in loading effects, insert a test voltage V_t, and observe how much signal returns (V_r). The loop gain then is defined as

$$T = \frac{V_r}{V_t} \quad . \tag{3.36}$$

Referring to Fig. 3.11, T is calculated in the following matter:

a) The loop is broken at the input of the dependent current source, leaving the integrator in a closed loop form.

b) Inserting a test voltage V_t and observing the voltage returned.

The circuit used for stability analysis is shown in Fig. 3.13. The open loop gain of the operational amplifier used at the integrator is 10^4.

The transfer function for loop gain analysis can be interpreted as (Refer to Fig. 3.13)

$$T = \frac{V_1}{V_t} \frac{V_r}{V_1} \tag{3.37}$$

where

$$\frac{V_r}{V_1} \simeq - \frac{Z_{int}}{R_2} \tag{3.38}$$

and

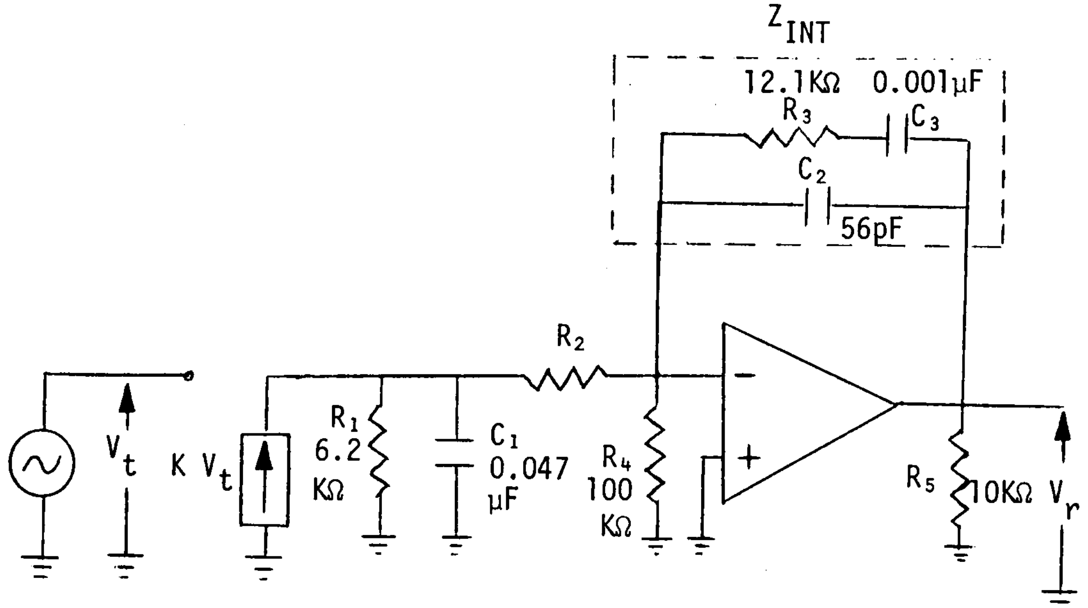

Figure 3.13. Circuit used for stability analysis

$$\frac{V_1}{V_t} = K\ (R_1||R_2||\frac{1}{sC_1}) = \frac{K(R_1||R_2)}{1 + sC_1(R_1||R_2)} \quad . \tag{3.39}$$

Substituting Eq. (3.39) into Eq. (3.38) gives

$$T = \frac{V_r}{V_t} = -\frac{K(R_1||R_2)}{R_2} \ \frac{Z_{int}}{1 + sC_1(R_1||R_2)} \quad . \tag{3.40}$$

The integrator impedance Z_{int} is calculated as

$$Z_{int} = (R_3 + \frac{1}{sC_3})\ ||\ \frac{1}{sC_2} = \frac{1 + sR_3C_3}{s(C_2 + C_3)(1 + s\ \frac{R_3C_2C_3}{C_2 + C_3})} \quad . \tag{3.41}$$

Substituting Eq. (3.41) into Eq. (3.40) in terms of jf yields

$$T = T_{mid}\ \frac{(1 + \frac{jf}{fz})}{jf(1 + \frac{jf}{fp_1})(1 + \frac{jf}{fp_2})} \quad , \tag{3.42}$$

where

$$T_{mid} = -\frac{K(R_1||R_2)}{2\pi R_2(C_2 + C_3)} \simeq -\ K(8.7988 \times 10^6) \quad , \tag{3.43}$$

$$f_z = \frac{1}{2\pi\ R_3C_3} \simeq 13.1\ \text{KHz} \quad , \tag{3.44}$$

$$f_{p1} = \frac{1}{2\pi\ C_1(R_1||R_2)} \simeq 580\ \text{HZ} \quad , \tag{3.45}$$

$$f_p = \frac{(C_2 + C_3)}{2\pi\ R_3C_2C_3} \simeq 247\ \text{KHz} \quad . \tag{3.46}$$

The frequencies f_z, f_{p1}, f_{p2} constitute the -3db critical frequencies of the pole-zero constellation of the loop transmission. The term jf in Eq. (3.42) is the critical frequency associated with the pole at s = 0 in Laplace form (pole at the origin).

It is interesting to note that different loop transmissions will be obtained for several values of C_p. This factor is introduced in the K term which is dependent on the output voltage (integrator) for each C_p affecting T_{mid}. However, the pole-zero constellation of T remains unchanged. These changes in T_{mid} are caused by the fact that K is a function of C_p and as C_p increases K will increase, therefore, increasing T_{mid} by the C_p factor. Table 3.1 shows the important points from the Bode analysis found using a computer program (see Appendix A).

Figure 3.14 shows the Bode plot of T and the phase vs C_p values of 1pF, 10pF, and 100pF.

The loop transmission was also found using computer analysis (PCAP) in the IBM 360/65 (see Appendix B). These results are shown in Fig. 3.15. Results from computer analysis and Bode analysis agreed.

As expected, the pole-zero constellation of T defines the stability of the system. Chapter 5 will mention how changes in the poles and zero causes certain changes in the closed-loop frequency response.

3.6. Closed-Loop Frequency Response Calculations

The closed-loop transfer function of the Roberts loop for the impedance measurement can be expressed by

$$A_{cl} = -\frac{V_{out}}{C_p} \quad . \tag{3.47}$$

TABLE 3.1. Important Points in the Loop Transmission Found with the Computer

C_p	V_{out}	T_{mid}	f_z	f_{p1}	f_{p2}	PM
1.0pF	10.0V	63.5081dB	13.140KHz	579.47Hz	247.79KHz	37.7°
10.0pF	1.0V	83.5081dB	13.140KHz	579.47Hz	247.79KHz	23.90°
100.0pF	0.10V	103.5081dB	13.140KHz	579.47Hz	247.79KHz	39.4°

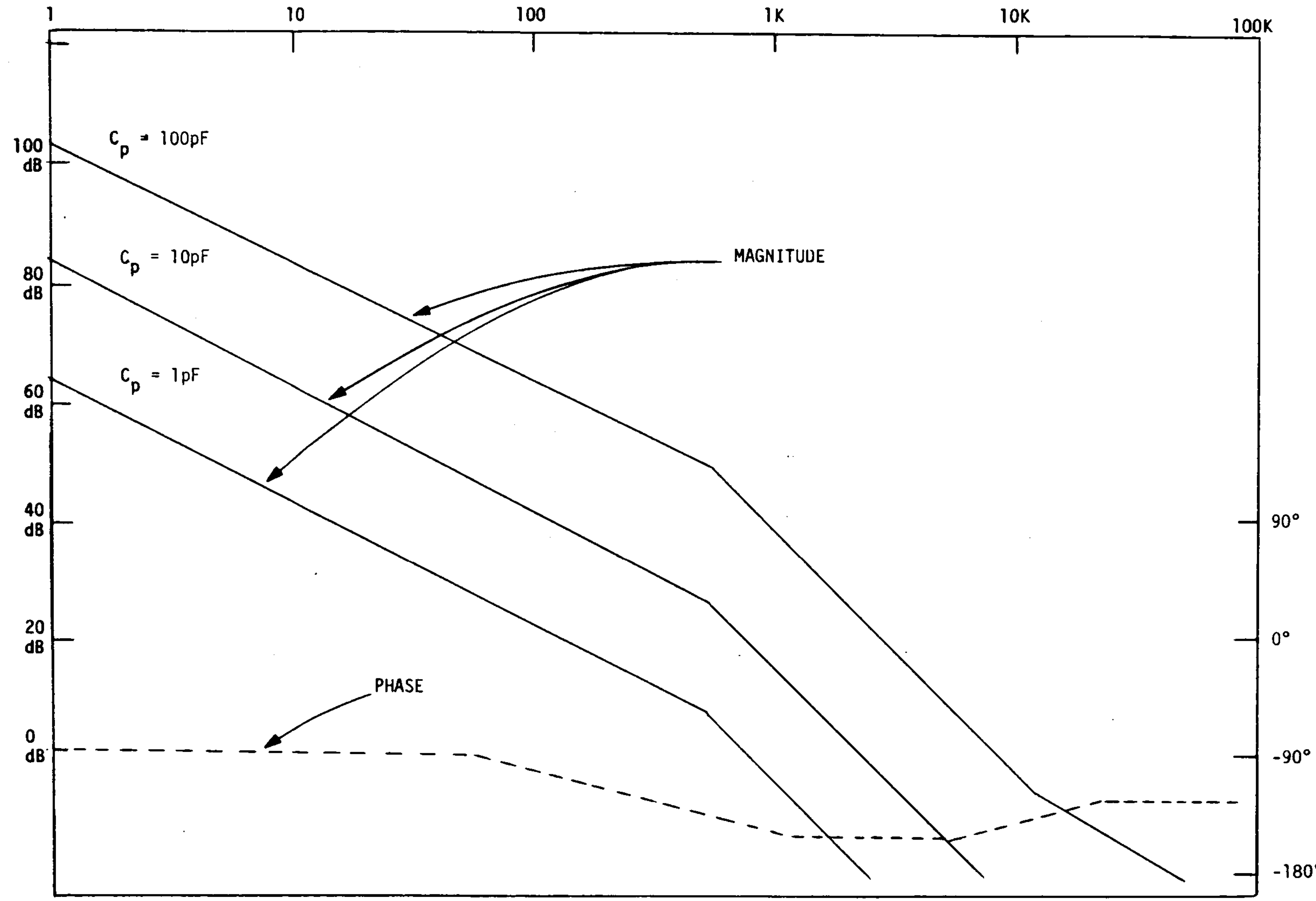

Figure 3.14. Bode plot of the loop transmission

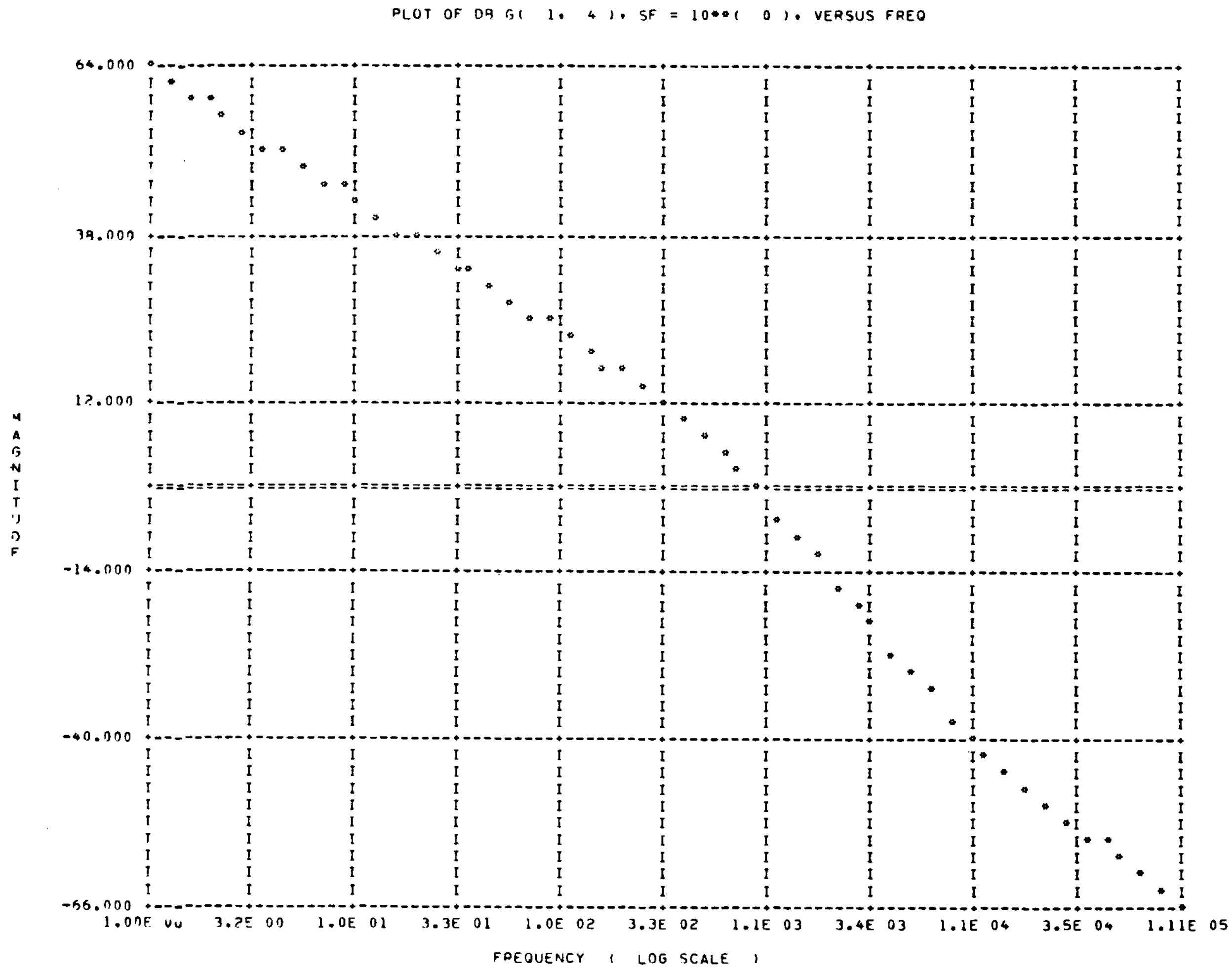

(a) $C_p = 1.0$ pF

Figure 3.15. Computer analysis of loop transmission

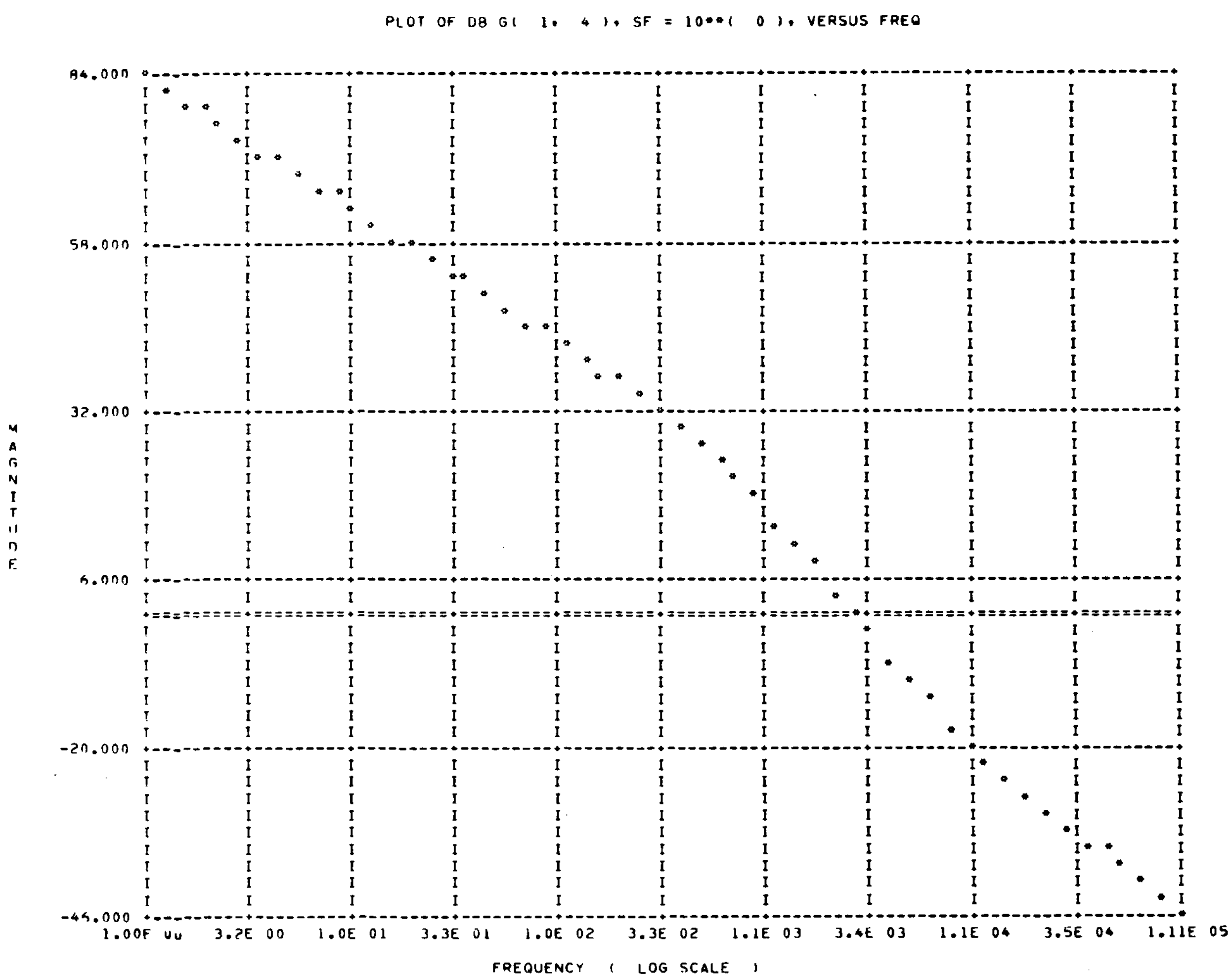

(b) $C_p = 10.0$ pF

Figure 3.15. (continued)

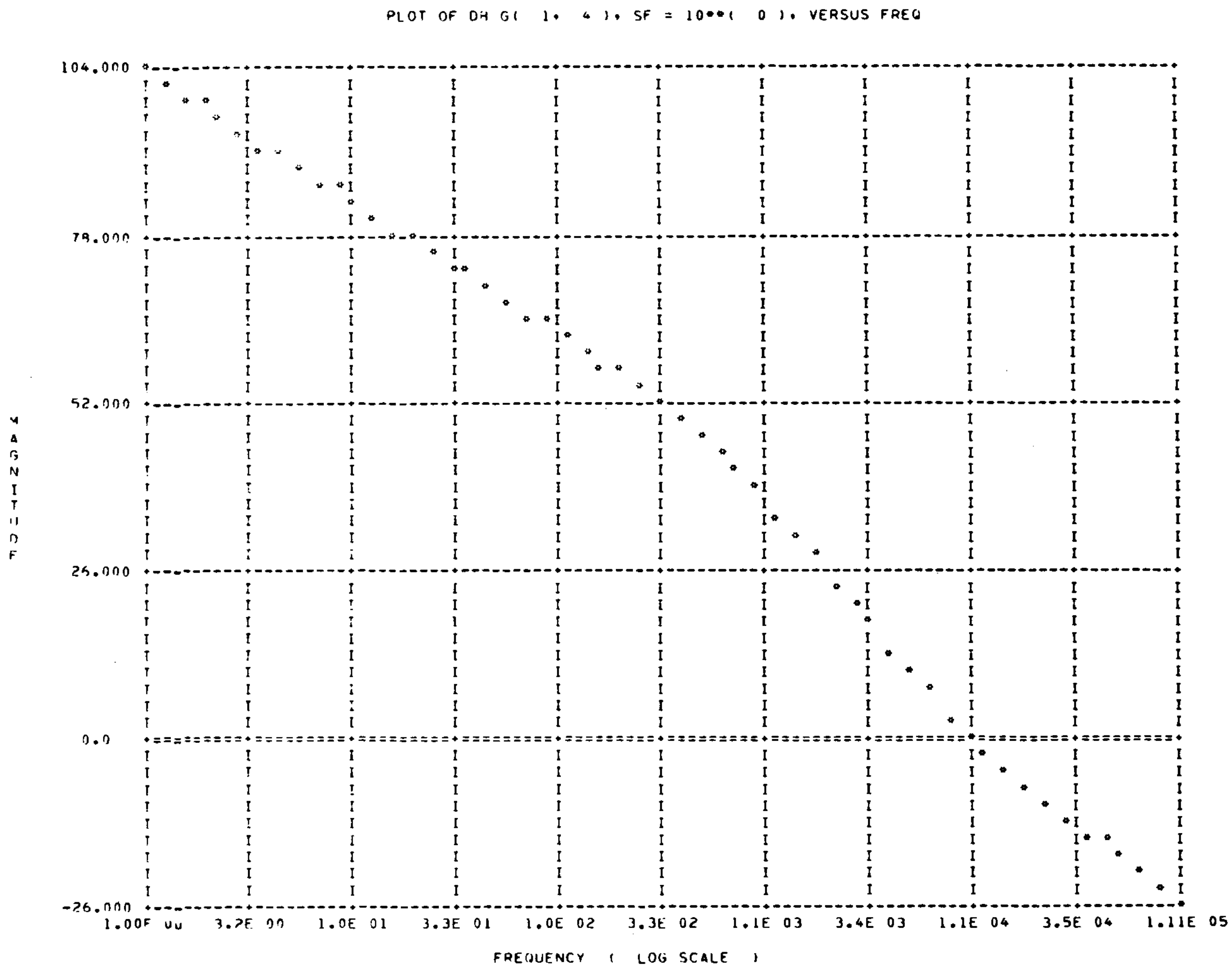

(c) $C_p = 100.0$ pF

Figure 3.15. (continued)

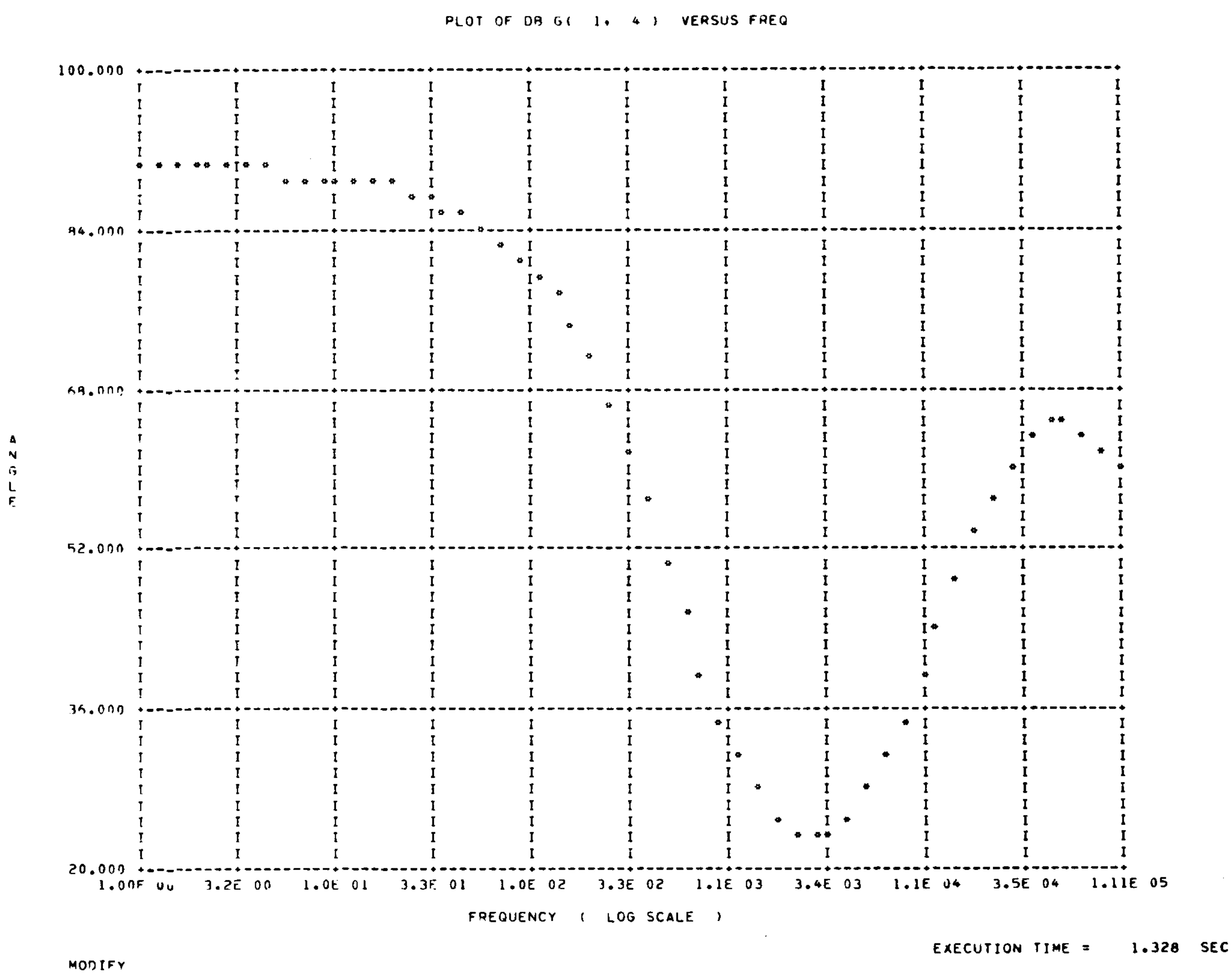

(d) Phase shift

Figure 3.15. (continued)

However, finding this unusual form is difficult, due to the fact that an impedance measurement is being taken in the feedback loop.

The idea behind the development of the model is to obtain a transfer function that uses an electrical signal equivalent to a probe impedance change. Once this is accomplished, all methods of circuit analysis can be used to calculate the system performance.

Several methods of introducing the electrical signal can be used. For example, the injection of current into the preamplifier, or the use of two electrodes, which have a certain value of capacitance, having a moving part between the electrodes controlled by a motor. This motor could change the capacitance as the speed of the motor, which controls the moving part, is increased. However, the implementation of these methods can be difficult. Alternatively, the insertion of a voltage source could be used to measure a transfer function which could be then analysed using standard feedback system analysis. The place to introduce the voltage source must be carefully considered. The voltage source can be placed at any point in the network and a transfer function obtained; however, the most logical place to introduce it would be at the dc set point (V_{set}). At the V_{set} point it would also be possible not just to compute closed-loop response, but also to implement transient responses equivalent to changes in probe capacitance. Using the approach of the voltage source at the set point makes easier experimental calculations and computer analysis; consequently, this method was used. Figure 3.16 shows the closed-loop model of the Roberts loop. The closed-loop response can be described by

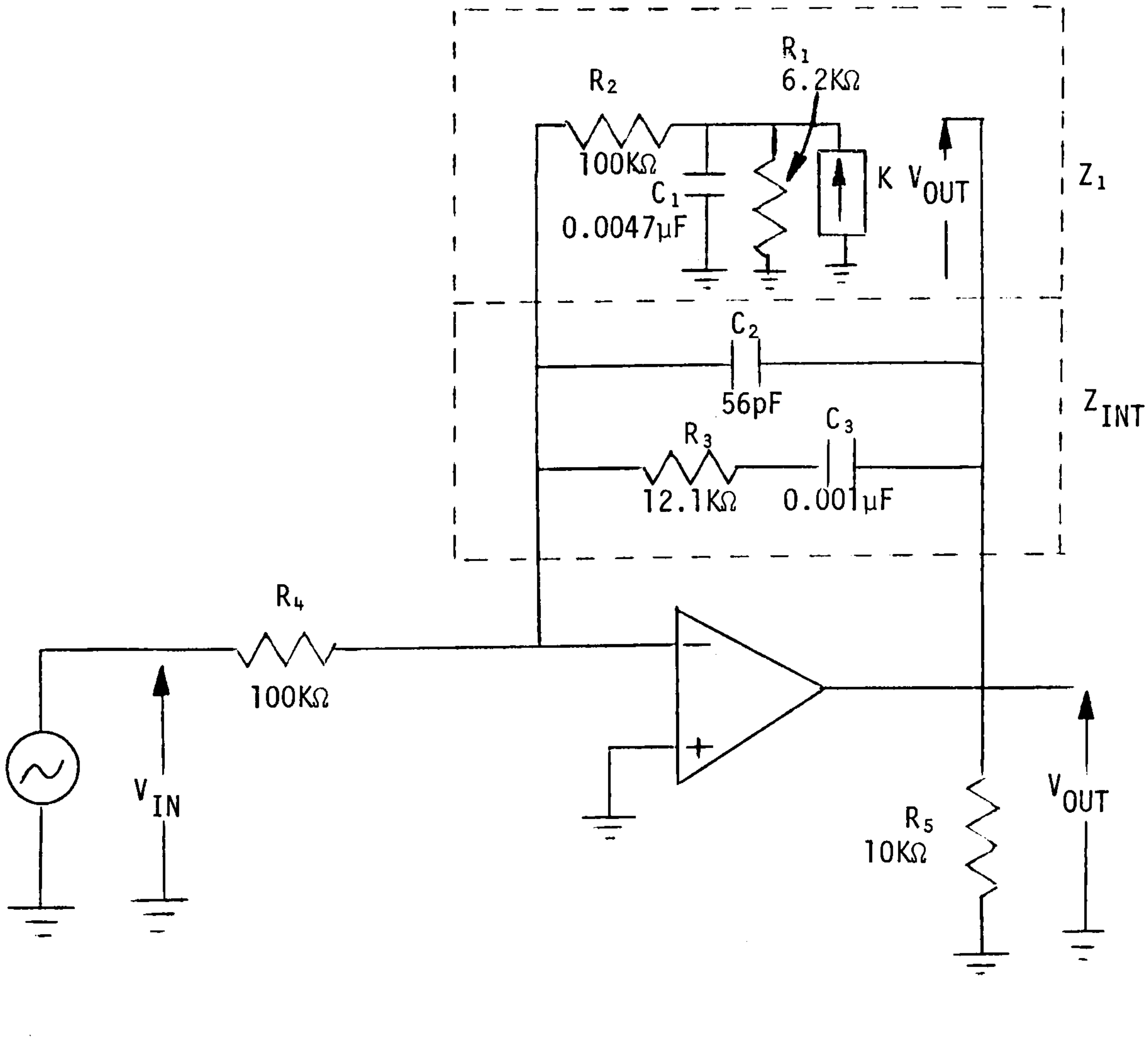

Figure 3.16. Closed-loop model of the Roberts loop

$$A_{cl} = \frac{V_{out}}{V_{in}} = -\frac{Z_1||Z_{int}}{R_4} \quad , \tag{3.48}$$

where Z_1 is the probe circuit transfer impedance and Z_{int} is the integrator impedance.

The probe circuit impedance, Z_1, can be calculated in (refer to Fig. 3.17) the frequency domain as

$$Z_1 = \frac{V_{out}}{i_{f1}} = \frac{R_2}{K(R_1||R_2)}\left(1 + \frac{jf}{f_{z1}}\right) \tag{3.49}$$

where f_{z1} is the critical frequency associated with the Laplace domain zero. The frequency f_{z1} is

$$f_{z1} = \frac{1}{2\pi \cdot C_1 \cdot (R_1||R_2)} \quad . \tag{3.50}$$

The integrator network (Z_{int}) is given by

$$Z_{int} = \frac{V_{out}}{I_{f1}} = \left(R_3 + \frac{1}{sC_3}\right)||\frac{1}{sC_2} = \frac{1}{2\pi(C_2 + C_3)} \; \frac{\left(1 + \frac{jf}{fz_2}\right)}{jf\left(1 + \frac{jf}{fp_2}\right)} \tag{3.51}$$

defined before by Eq. (3.44), (3.45), and (3.46).

Substituting Eq. (3.51) and Eq. (3.49), after algebraic manipulation, into Eq. (3.48) we get

$$A_{cl} = \frac{-\left(1 + \frac{jf}{fz_1}\right)\left(1 + \frac{jf}{fz_2}\right)}{[R_2(2\pi)(C_2 + C_3)]\; jf\left(1 + \frac{jf}{fp_1}\right)\left(1 + \frac{jf}{fp_2}\right) + K(R_1||R_2)\left(1 + \frac{jf}{fz_2}\right)} \;, \tag{3.52}$$

Assuming $A^{OpAmp} = \infty$, $Z_{in}^{OpAmp} = \infty$, and $R_0^{OpAmp} = 0$.

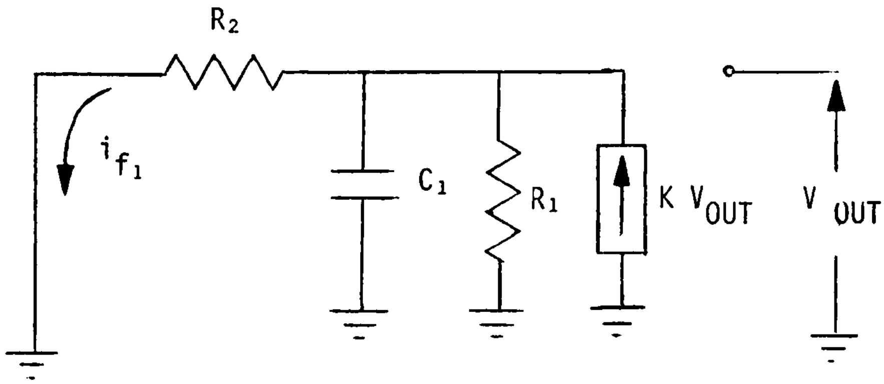

Figure 3.17. Circuit for the calculation of probe impedance

Equation (3.52) represents the closed-loop transfer function (in frequency space) approximation for the Roberts loop model. Due to its complexity, the electronic signal processor was simulated using a digital computer (PCAP program, IBM 360/65), where the frequency response was obtained for different values of C_p (1pF, 10pF, and 100pF). These plots will be shown in the next section with the experimental results.

3.7. Experimental Closed-Loop Response

The closed-loop response (A_{cl}) of this electronic system differs greatly in comparison to most ordinary feedback system, due to the fact that a parameter (C_p) in the feedback path is changing and, consequently, creating different A_{cl} responses. In the model the change is accounted for in the K term.

Frequency response of the closed-loop system was taken by inserting a sinusoidal wave at the set point and observing the output voltage such that

$$A_{cl} = \left| - \frac{V_o}{V_{in}} \right| \text{ or } A_{cl} = 20 \log |A_{cl}| \qquad (3.53)$$

The theoretical closed-loop response was calculated by the computer with a sine wave input at the set point (see Appendix C).

Figure 3.18 shows how the bias level was maintained at the set point. Results of the experimental and calculated closed-loop gain are plotted and shown in Fig. 3.19 for values of C_p equal to 1pF, 10pF, and 100pF.

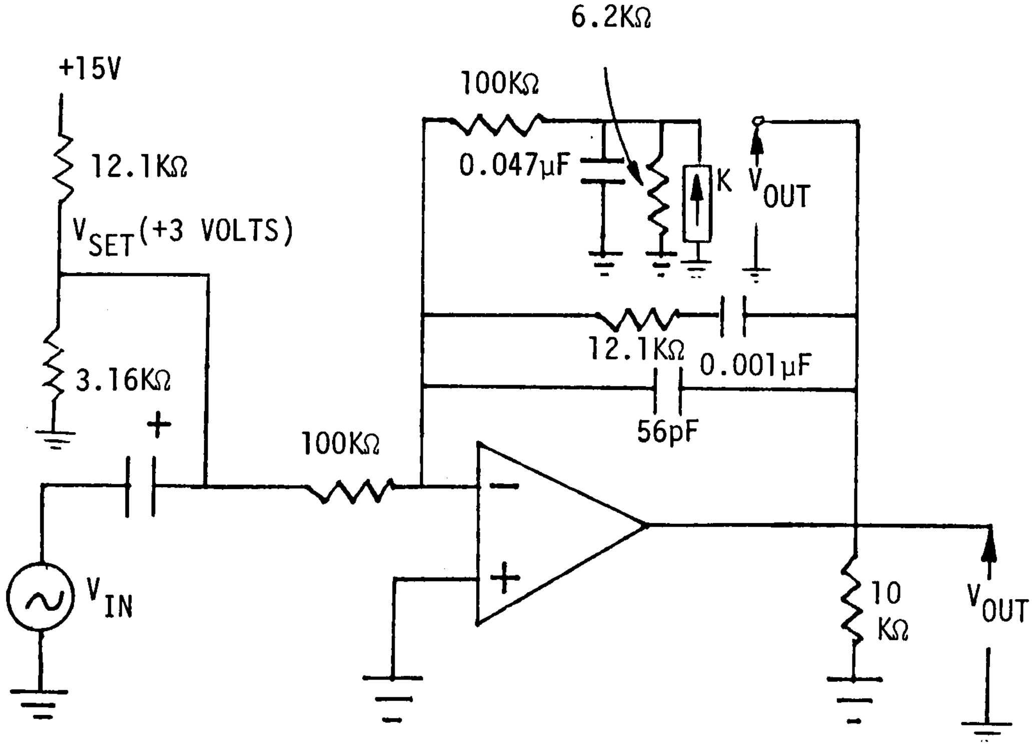

Figure 3.18. Bias level at set point in experimental closed-loop response

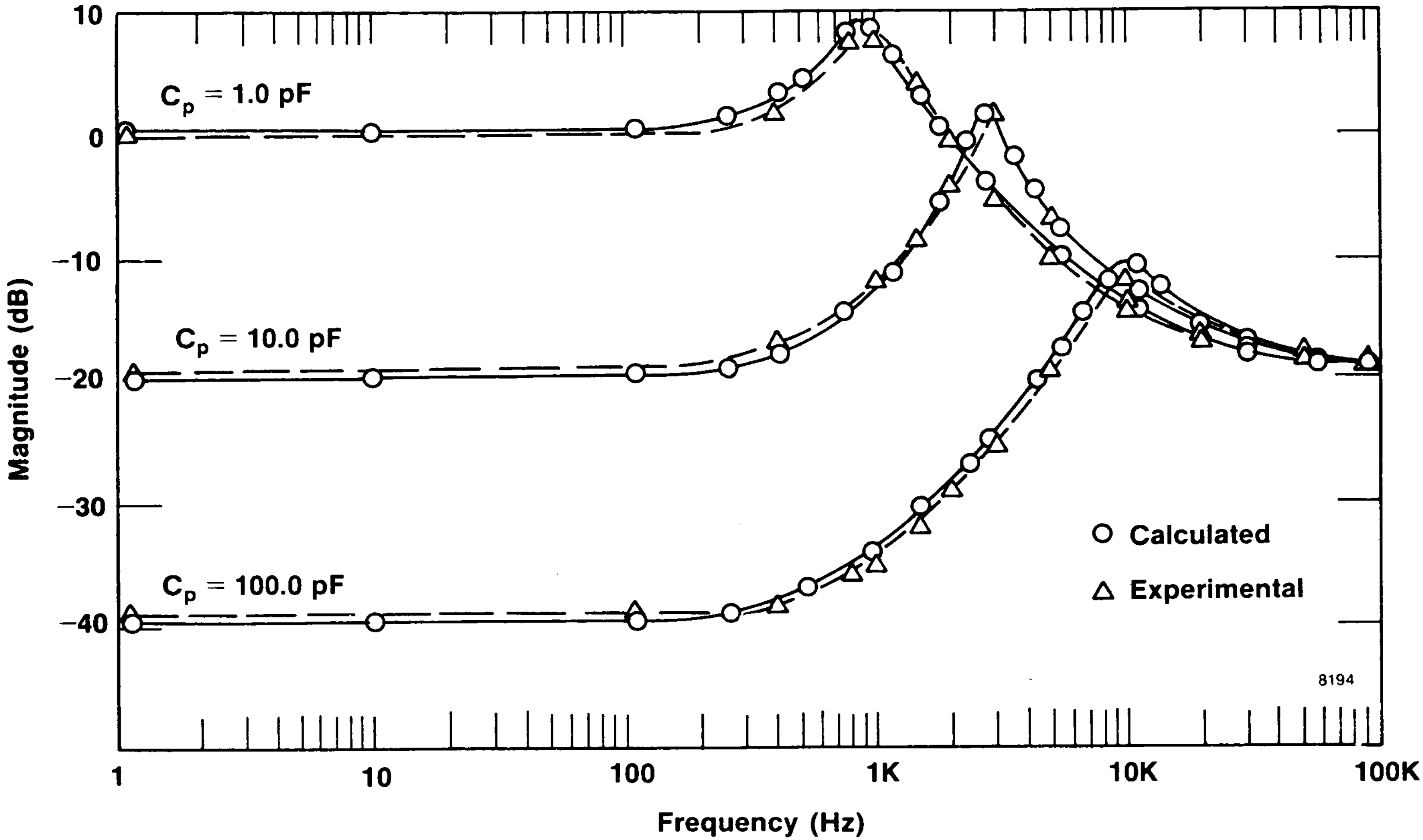

Figure 3.19. Experimental and calculated closed-loop frequency response

Referring to Fig. 3.19, the frequency response can be divided into three different regions. The first one being the linear region that extends in this case to about 200Hz, the second region composed of the peaking in the response, and the third one the high frequency region for the system (beyond 30 KHz).

The linear region, the peaking in response, is caused by the loop transmission. The cross-over frequency, f_c, and the phase margin will determine the amount of peaking observed and its frequency location. Note that the closed-loop transfer function is not a pure second order approximation.

The third region is defined by the gain at high frequency. This gain is defined by R3/R4 in Fig. 3.2, on page 10.

Results from calculated (computer analysis), and experimental responses were very close for this unusual type of frequency response.

3.8. Summary

A general description of the Roberts loop has been presented in this chapter and the approximation made to derive the model used for analysis was justified. Using the model, oscillation stability analysis was performed and, both calculated and experimental closed-loop frequency response functions were generated.

CHAPTER 4

TRANSIENT ANALYSIS AND SYSTEM PERFORMANCE

4.1. Introduction

The objective of this chapter is to present the method used to obtain the transient response of the system. This transient response was based on the model developed. Results from a matching method used for calculating the transient response are also presented. The performance of the system is included to show how linearity and sensitivity of the signal processor is effected by changes in probe capacitance. All of this experimental work was performed in laboratory tests at E. G. & G. Oak Ridge Operations.

4.2. Transient Response Analysis

The transient response for the AIRS electronic signal processor will show how fast the output can follow the change in probe capacitance. However, according to the model developed, a similar response must be obtained from a voltage change at the set point (V_{set}). This test on transient matching, from a ΔC_p to a ΔV_{set}, will enable us to predict the response for any change in component value when optimizing the system. It will also prove the validity of the model, since an electronic system can be disturbed at any point in the network to create a transient. This transient, though, must be interpreted in the correct manner. A step change in capacitance, ΔC_p, is difficult to implement; therefore, C_p changes are obtained by switching a known ΔC_p with a relay in parallel with C_p. Figure 4.1 shows this arrangement. When the relay is OFF the capacitance is C_p, and when the relay is switched ON the capacitance is $C_p + \Delta C_p$, thus incrementing C_p by ΔC_p. Due to the time required by the armature of the relay to close (delay), an RC network was introduced at the set point to modify the rise time of ΔV_{set} to simulate the relay delay.

To match a transient response for the model (voltage-to-voltage), a step change in V_{set} (d.c. set point) will be used. This step change will create a transient and the value of ΔV_{set} will match a certain value of ΔC_p which cause the same response. The theoretical transient response was implemented using PCAP transient analysis in the IBM 360/65 computer. The RC network was placed at the input of the model at the set point (V_{set}) [3]. The value of this RC time constant was found experimentally when matching ΔC_p and ΔV_{set} transients. The theoretical transient response also used the RC network to obtain the calculated transient; this is shown in Appendix C. Note that this is a small-signal analysis so that T does not change much during the ΔC_p excursion.

4.3. Measurement Scheme and Transient Response

For transient response measurement very accurate values of capacitance were needed. Probe capacitance measurements were performed with a direct capacitance bridge (Booton Electronics model), where all stray capacitance was included. Values of ΔC_p (change in C_p) were approximately 10% of the probe capacitance (C_p). These changes, ΔC_p,

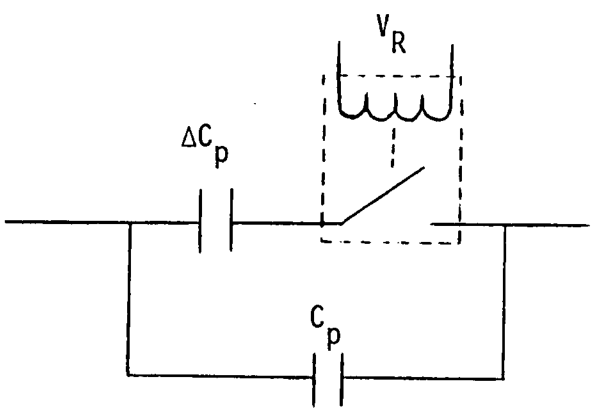

Figure 4.1. Arrangement used to create ΔC_p

were taken with the relay in the ON and OFF states, thus, allowing data readings of (C_p + ΔC_p) to be accurately obtained.

Figure 4.2 shows a complete block diagram of the scheme used to measure the transient response of the system.

Testing was simplified by synchronizing the relay drive with the system clock (oscillator). This synchronization was accomplished with the use of discriminators and divide by 1000 pre-scalar [3]. Figure 4.3 shows a block diagram of the setup. The input to the discriminator was the 100 KHz oscillator. The purpose of this discriminator was to provide a negative logic pulse when the trailing edge of the sine wave crossed zero. The divide by 1000 pre-scalar was used to set the triggering frequency at 100 Hz. The output voltage of the pulse generator was the voltage used to switch the relay that provided the C_p changes.

When testing transient response, changes in C_p occur from switching the relay with V_r; these responses were the actual transients of the system.

To perform experimental analysis based on the model developed, the square wave from the pulse generator was used to provide a ΔV_{set} (step change in V_{set}) at the d.c. set point. The RC time constant was incorporated in the circuit to provide the necessary rise time (τ_r) for the signal ΔV_{set} to compensate for the relay delay time (τ_d).

The transient match was approximated by finding a particular value of ΔV_{set} which would cause the same transient response with ΔC_p. To maintain the set point at +3 volts d.c., baseline restoration was used

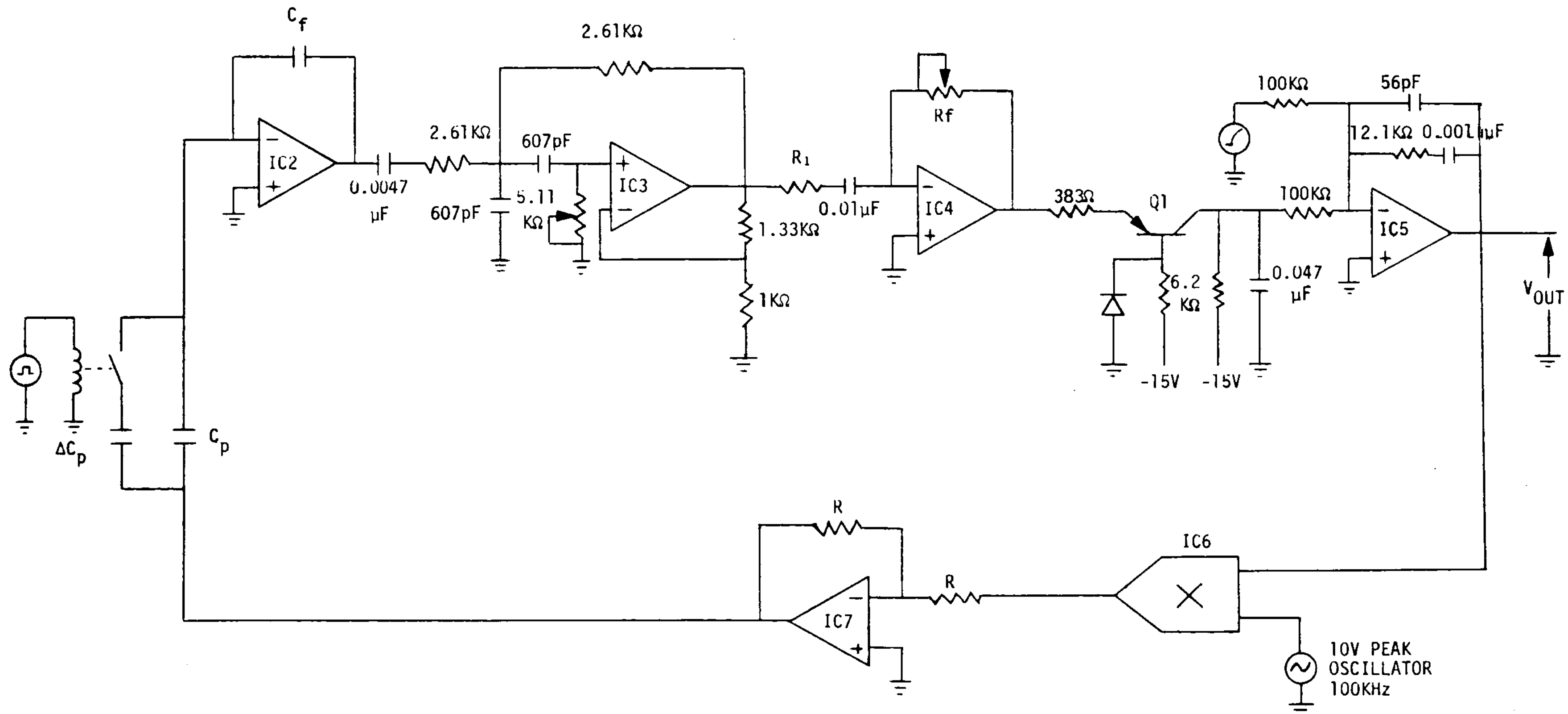

Figure 4.2. Complete block diagram of the scheme used to measure the transient response of the system.

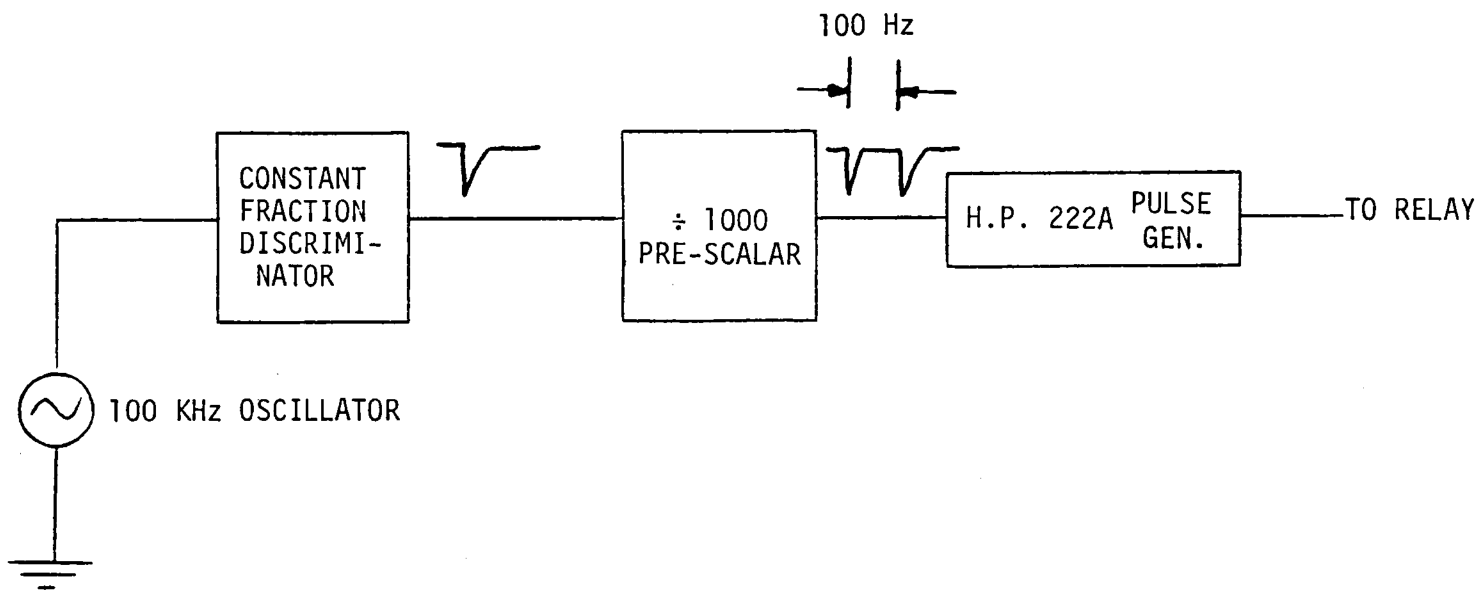

Figure 4.3. Circuit for triggering the relay

[10]; this was accomplished easily with the use of a Germanium diode. Figure 4.4 shows the arrangement used to provide baseline restoration and the RC network.

Results from transient analysis are shown in Fig. 4.5. Picture (a) shows the transient obtained by switching 0.401 pF (ΔC_p) parallel to a probe capacitance of 3.896 pF. Note the down excursion of the transient due to the relay closing time (approximately 85 usec). Picture (b) shows the ΔV_{set} voltage applied to obtain a similar transient response as (a); as can be seen, the rise time of ΔV_{set} (550 μsec) was needed. Picture (c) shows a superposition of the two transient responses which illustrates excellent matching. The calculated transient response obtained through PCAP analysis is shown in part (d) using a ΔV_{set} change at the d.c. set point.

Table 4.1 shows the results in a tabulated form for several capacitance values. It is interesting to note (refer to Table 4.1) that the rise time increased as the percentage overshoot decreased for probe capacitance values ranging from 10.85 pF (ΔC_p = 0.97 pF) to 2.85 pF (ΔC_p = 0.247 pF) respectively. This is expected since there are different loop transmissions and closed-loop responses for each value of C_p.

Table 4.1 compares the different determinations of the output voltage, percentage overshoot, and rise times. The rise time calculated from f_c was taken from Pierce and Paulus [8].

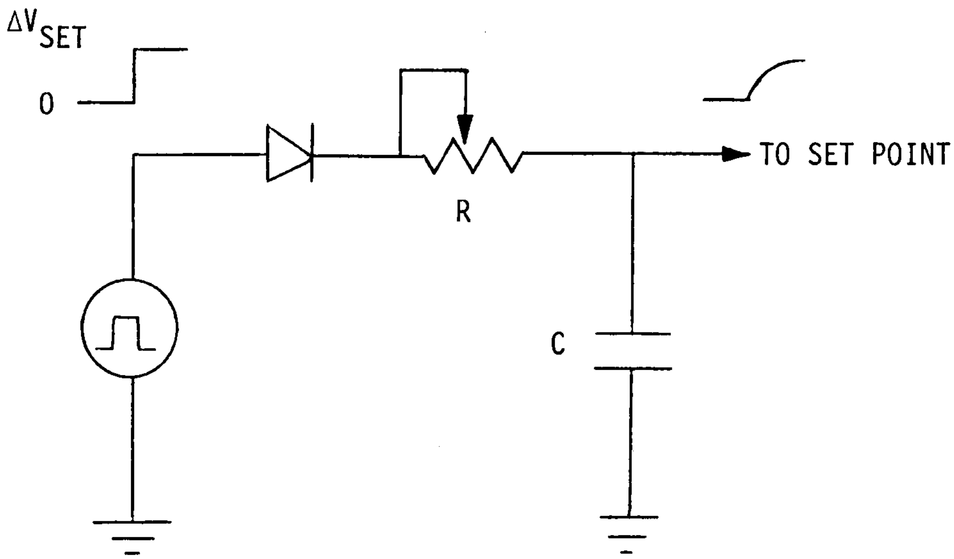

Figure 4.4. Baseline restoration and RC network

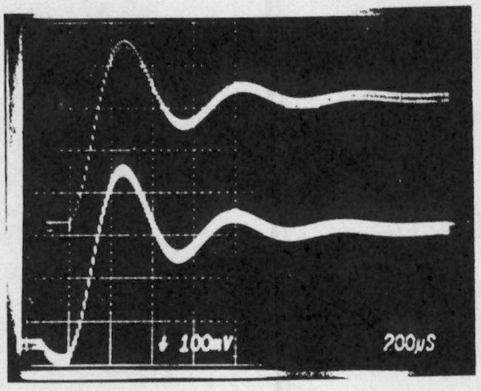

C_p = 3.896 pF
ΔC_p = 0.401 pF

(a)

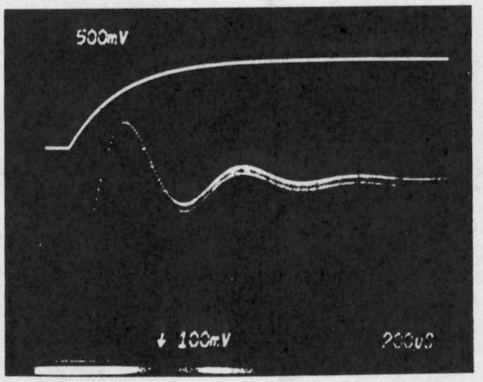

(b)

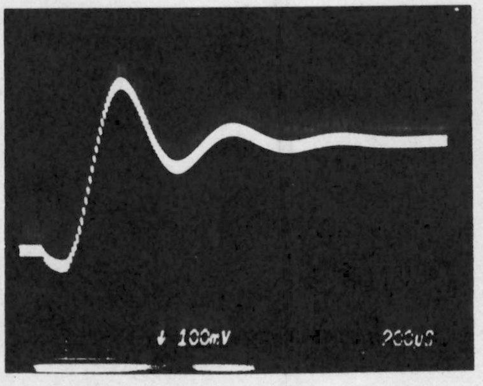

(c)

Figure 4.5. Results from transient analysis

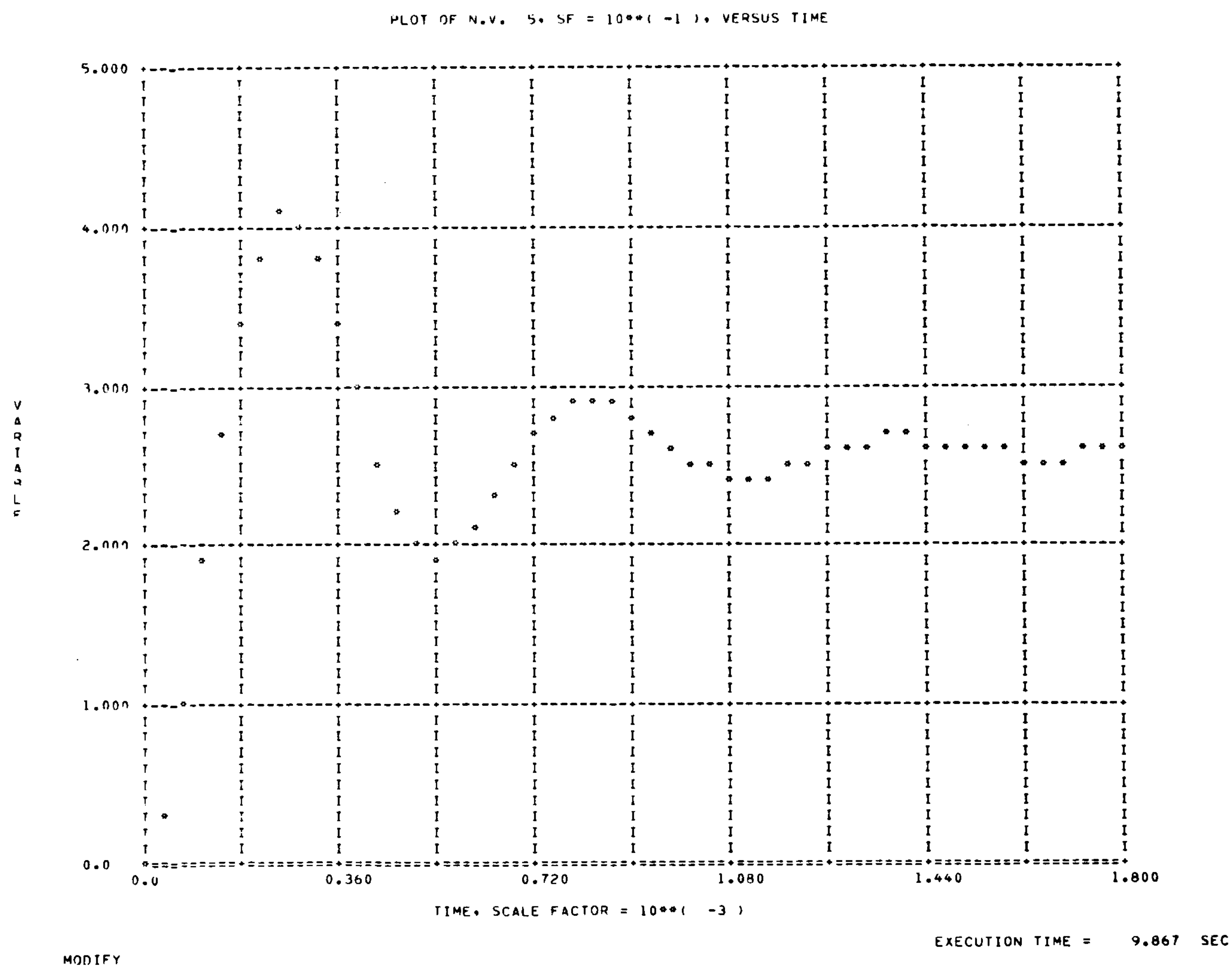

(d)

Figure 4.5. (continued)

TABLE 4.1. Transient Result for Several Probe Capacitance Values

C_p (pF)	ΔC_p (pF)	$V_{(OUT)}$ CALCULATED (VOLTS)	V_{OUT} EXP. (VOLTS)	ΔV_{OUT} (mV)	dV/dCp (V/pF)	τr TRANSIENT EXP. (OUTPUT) μSEC	τr TRANSIENT COMPUTER (OUTPUT) μSEC	τr FROM f_c	% O.S. EXP.	% O.S. CALCULATED COMPUTER	ΔV_{SET} (VOLTS)	τr OF ΔV_{SET} (μSEC)
10.85	0.47	0.922	0.966	101	0.1041	50	54	54.26	64.51 %	62.775%	1.53	550
7.7	0.716	1.2987	1.3714	120	0.1684	70	68	66	63.8 %	62.21 %	1.26	550
5.828	0.662	1.7159	1.818	158	0.23867	90	86	78	60.869%	61.8 %	1.12	550
3.896	0.401	2.5667	2.761	266	0.66334	110	97	98.4	57.575%	57.24 %	1.0	550
2.85	0.247	3.508	3.853	318	1.28745	130	126	120	52.63 %	52.89 %	0.89	550

4.4. System Linearity and Sensitivity

Results of the analysis of AIRS Electronic System show that the output is proportional to $|Z_p|$ or $|\frac{1}{C_p}|$. Tests for linearity were done by calibrating the system to 10 volts output for a C_p value of 2.493 pF and 0.12 volts output for C_p of 207.7 pF. This calibration was performed to make the output voltage pass through zero volts for $|Z_p|$ equal to zero. The value of 2.493 pF constitute C_{pmin}. The output voltage, as mentioned before, is inversely proportional to C_p, therefore, V_{out} can be expressed by [11]

$$V_{out} = \frac{H}{C_{pmin}} \quad , \tag{4.1}$$

where H is the proportionality constant and C_{pmin} the probe capacitance used for an output voltage equal to 10 volts.

Figure 4.6 shows the relationship of C_p versus the output voltage. For this case, H is equal to 24.93 from Eq. (4.1). The range of error for five units in percent of reading is shown in Fig. 4.7 for probe capacitance changes over a 176:1 dynamic range.

Sensitivity of the system to changes in probe capacitance is proportional to $1/C_p^2$. Figure 4.8 shows the sensitivity of the system. The AIRS Electronic System is most sensitive to small changes in probe impedance at very high values of void fraction. This sensitivity $(1/C_p^2)$ proportionality an be calculated as $|dV/dC_p|$, and is derived from

$$V_{out} = \frac{H}{C_{pmin}} \quad , \tag{4.2}$$

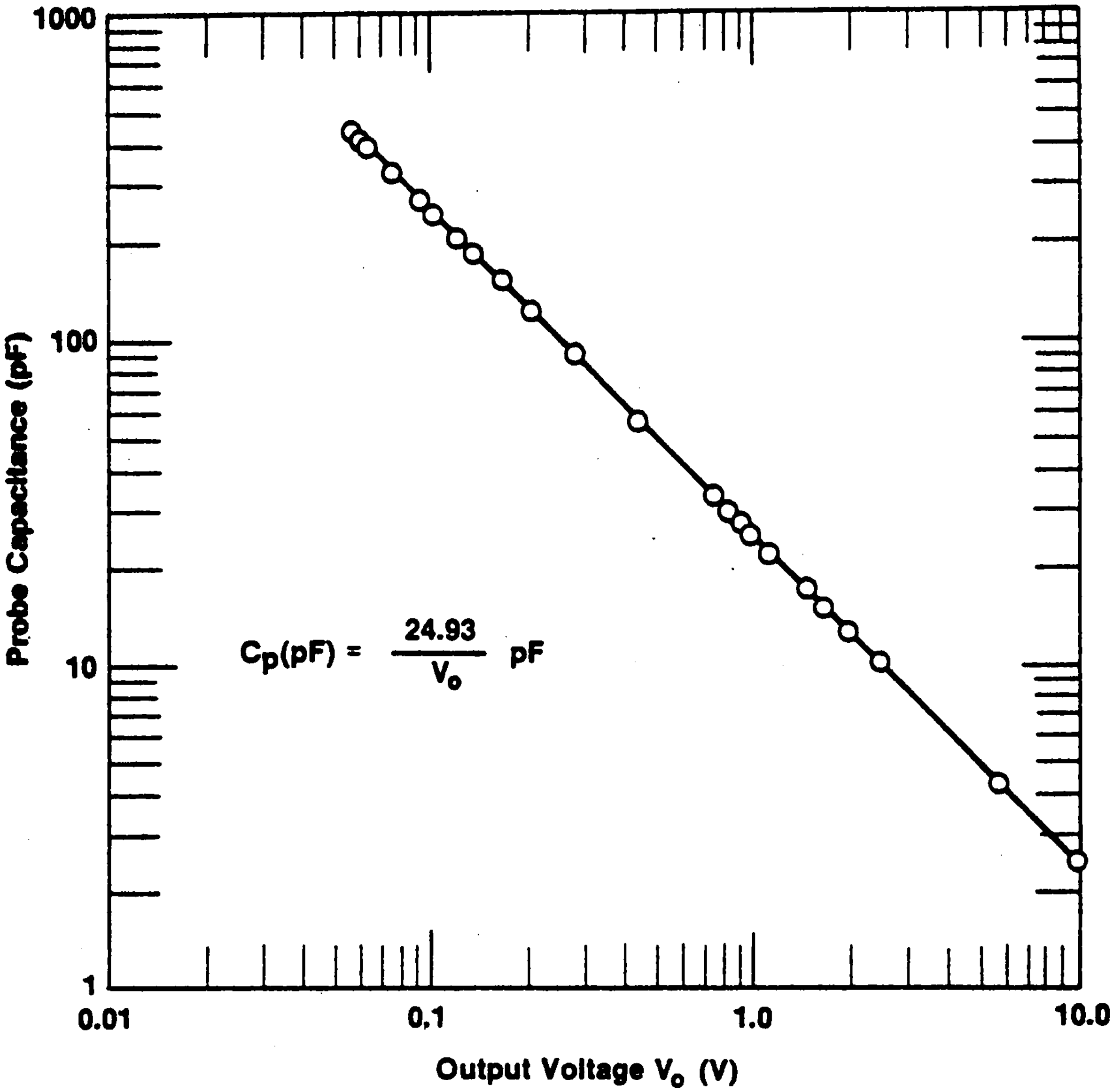

Figure 4.6. Linearity with H = 24.93 (Courtesy of E. G. & G. Operations)

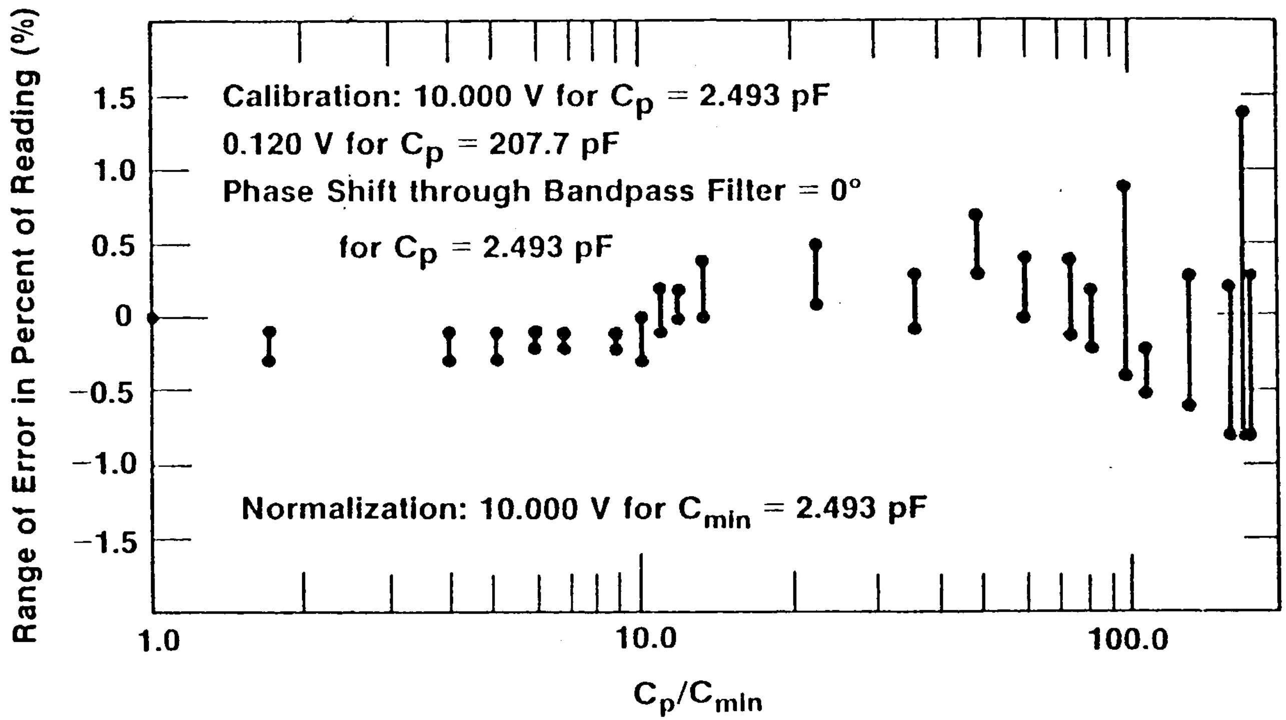

Figure 4.7. Range of percent error in reading with five units (Courtesy of E. G. & G. Oak Ridge Operation)

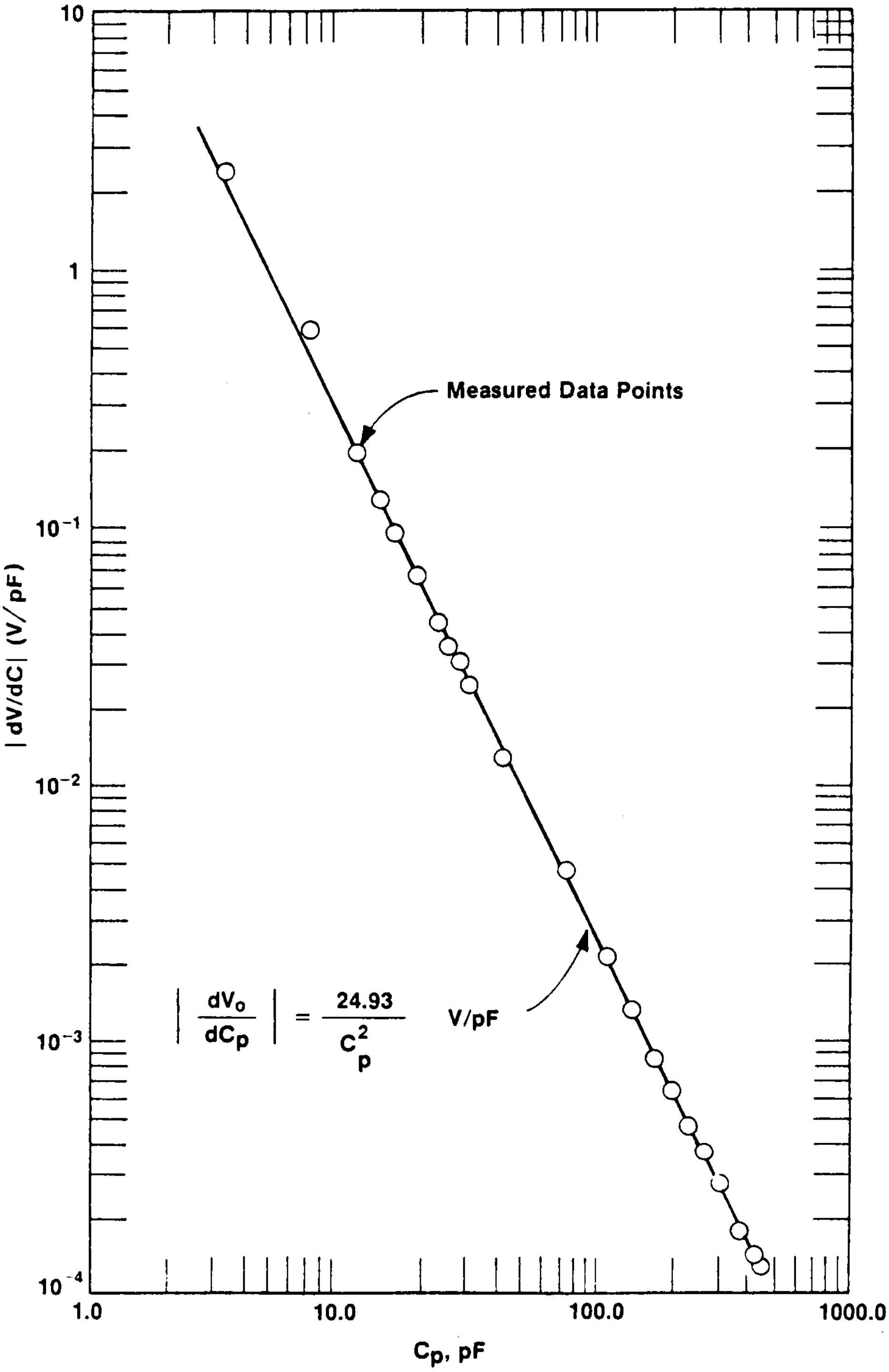

Figure 4.8. Sensitivity of the system (Courtesy of E. G. & G. Oak Ridge Operation)

so

$$dV_{out} = -\frac{H}{C^2_{pmin}} \quad dC_{pmin} \quad , \tag{4.3}$$

then

$$\left| \frac{dV_{out}}{dC_{pmin}} \right| = \frac{H}{C^2_{pmin}} \quad , \tag{4.4}$$

where H is the constant used for calibrating the system.

As can be seen, the output voltage (V_{out}) is proportional to $1/C_p$, where the constant H sets the desired V_{out} for a particular C_{pmin}. The value of H is defined by the variable gain stage (Ag).

4.5. Summary

In this chapter the scheme used to perform the transient experiments was presented. Results from matching transients for ΔC_p and ΔV_{set} are also shown. Sensitivity and linearity were also presented for a minimum probe capacitance value which was used for calibrating the system. These results prove the validity of the model.

CHAPTER 5

OPTIMIZATION CONSIDERATIONS

5.1. Introduction

This chapter will present the important details to take into consideration when optimizing the AIRS Electronic System for a particular application. These details are based on the analysis previously done.

5.2. Considerations for Desired System Response

The signal processor model will allow the determination of a desired closed-loop response bandwidth and the trade-offs that must be made. Transient response can be predicted from loop transmission calculations for any changes in parameters which lead to optimization.

In Chapter 3, the expression for the loop transmission, T, was derived and shown to have the form

$$T = T_{mid} \frac{(1 + \frac{jf}{fz})}{jf(1 + \frac{jf}{fp_1})(1 + \frac{jf}{fp_2})} \quad . \tag{5.1}$$

From experimental and calculated closed-loop response, peaking can be observed to occur approximately at the 0d.B. crossover frequency (f_c) of T. This is characterized by an approximate second-order system. The pole location associated with f_{p_1} is created at the output of the rectifier-demodulation section with the RC network, where C is the filter capacitor that defines the ripple factor since R is fixed to determine the voltage at that point. Changes of C will move the pole location. This change in C will also cause a change in ripple voltage which must be considered due to the fact that the multiplier nonlinearities become significant at about 200 mV ripple in the modulating signal input (V_{out} of integrator).

The closed-loop gain at frequencies ranging from 50 KHz to 200 KHz appear at a gain of -19 dB approximately, caused by the 12.1KΩ resistor in the integrator's circuit. Parameters in the integrator feedback (Z_{int}) also determine the value of the loop gain, and careful choices must be made to keep the system stable. These parameters in Z_{int} also define a lead network given by f_z which improves the phase margin.

Table 5.1 shows how changes in component values will cause certain pole-zero locations to change.

To perform an optimization, the desired frequency response and speed of time response must be known, so that pole locations can be shifted properly. Linearity will also vary as a trade off in bandwidth since f_p primarily defines f_c. Note that a sixth order pole low pass filter is located at the output of the integrator (refer to Fig. 3.1, page 9) which has a cutoff frequency at 1KHz; therefore, the response seen at the output of this filter will not contain any signal beyond 1KHz in frequency.

Figure 5.1 shows the closed-loop response modified by placing a 1.21KΩ resistor in place of the 12.1KΩ and a 0.01μF capacitor instead of 0.001μF to keep the same zero location (f_z) of T. This change brings the gain to -39 dB at frequencies beyond 10 KHz.

TABLE 5.1. Changes in Pole-Zero Locations Due to Component Changes

CHANGES IN "T"	MODEL COMPONENTS					
	↑ R_1	↑ R_2	↑ R_3	↑ C_1	↑ C_2	↑ C_3
f_z			↓			↓
f_{p_1}	↓	↑		↓		
f_{p_2}			↓		↓	↓
T_{mid}	↑	↓			↓	↓

↑↓ Indicates a change in "T"

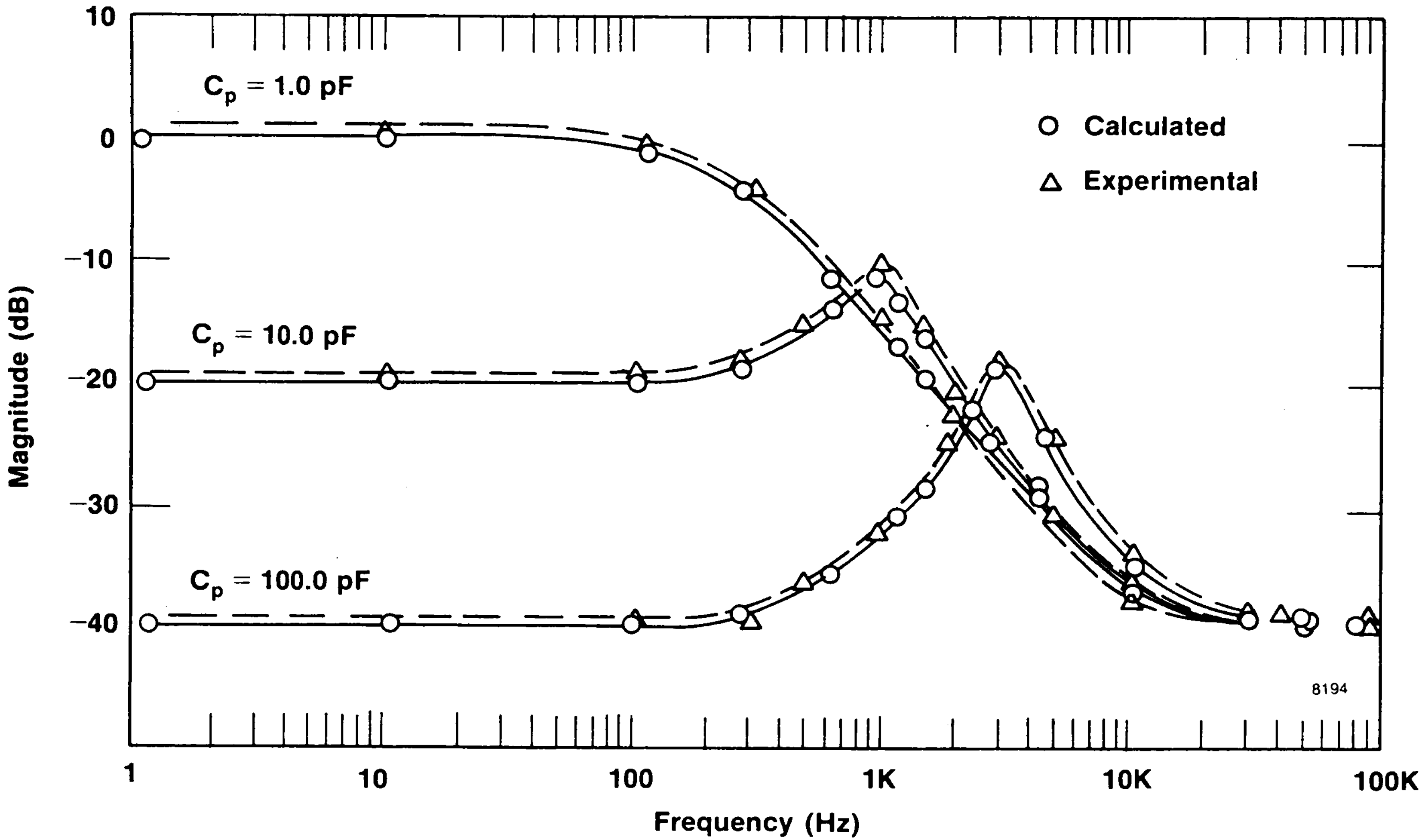

Figure 5.1. Modified closed-loop response

Figure 5.2 shows the possibility of increasing the bandwidth to about 1KHz with a ripple factor of approximately 100 mV. The filter capacitor was changed to 0.01μF, and the lead compensation capacitor from 1000 pF to 1500 pF.

It can be noted that the closed-loop response depends on several factors and trade-offs in linearity have to be made to achieve the desired response; this is primarily caused by the ripple factor at the rectifier section. Linearity tests were made for a 100:1 dynamic range of probe capacitance; however, an 80:1 range will improve the linearity since the nonlinearities were observed for high values of C_p [3]. Figure 5.3 shows linearity for compensation made with 200 mV ripple factor (bandwidth of 1KHz).

5.3. Summary

This chapter showed some considerations that must be taken into account when optimizing the system. Importance must be placed on the desired linearity and bandwidth of the system when dynamic range of operation is specified.

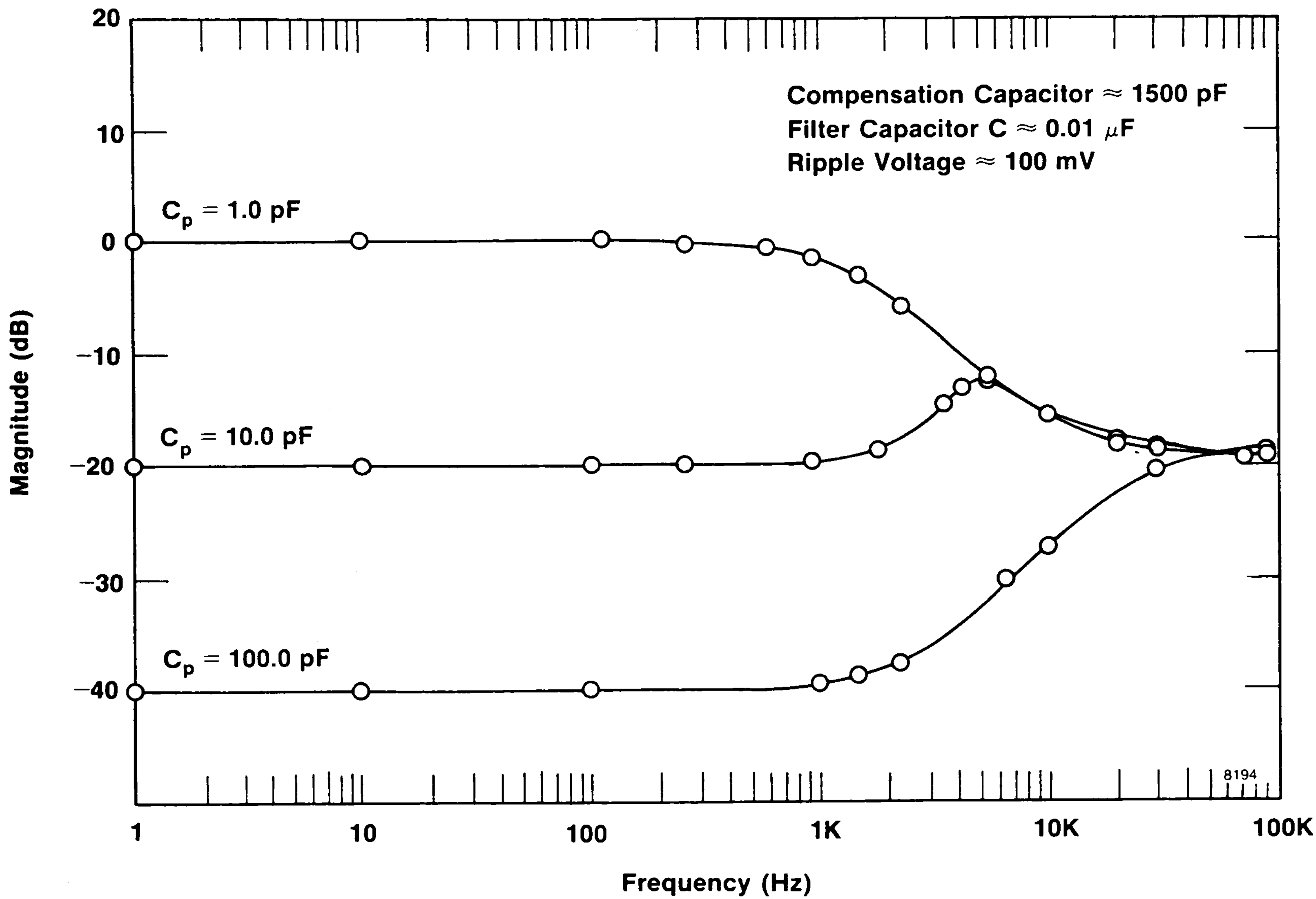

Figure 5.2. Closed-loop response with bandwidth of 1 KHz and ripple voltage of 100 mV

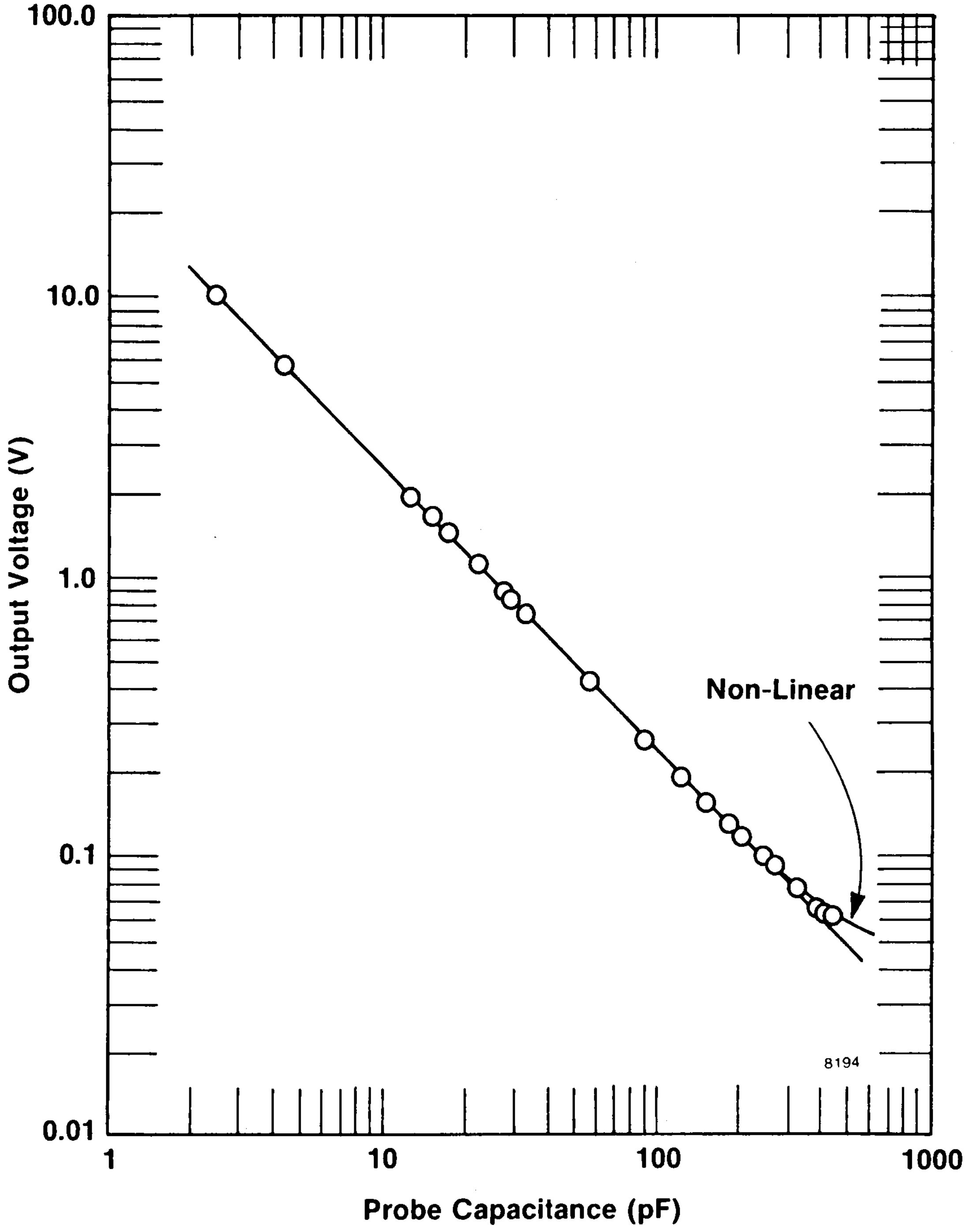

Figure 5.3. Linearity with ripple voltage of 200 mV and bandwidth of 1 KHz

CHAPTER 6

CONCLUSIONS AND SUGGESTIONS FOR FURTHER WORK

6.1. Conclusions

The work presented in this thesis leads a model of the AIRS Electronic signal processor which uses the Roberts loop. Based on this model, stability studies, transient analysis, and closed-loop frequency response were determined to understand how the system operates.

Results from experimental work show the validity of the model developed. Also, for any parameter change in the electronic system, a prediction of system response could be made. This response can also be experimentally tested using the measurement scheme described in Chapter 4.

6.2. Suggestions for Further Work

This model approximation is as based on the restriction that the sideband frequencies occur very close to the center frequency (100KHz); further analysis can be done to define the limits where these sidebands can be located in frequency space and still provide accurate results.

The $K\,e^{-S\tau}$ analysis could also be extended to determine how it affects the approximation of the model. The modulating section (multiplier) could be analyzed in more detail since a mathematical representation of its output is a real-time convolution of the two input signals.

The phase detection circuit was not included in this investigation and could also be studied in more detail.

Finally, depending on how specification requirements are placed, a desired system response can be achieved and studied taking in consideration the details pointed out in Chapter 5.

LIST OF REFERENCES

LIST OF REFERENCES

1. Advance Instrumentation for Reflood Studies (AIRS) Electronic System, Part A, AIRS Electronic System Characteristics, Second Report, July 1979.

2. E. W. Walker, "A Method for Reducing the Effect of Cable Capacitance on Admittance Measurements," M. S. Thesis, The University of Tennessee, Knoxville, Tennessee, 1979.

3. T. J. Paulus, Private Communications, E. G. & G. Oak Ridge Operations, Oak Ridge, Tennessee, 1979.

4. T. V. Blalock, Unpublished Research, Electrical Engineering Department, The University of Tennessee, 1979.

5. R. Coughlin, F. Driscoll, Operational Amplifiers and Linear Integrated Circuits, Prentice-Hall, New Jersey, 1977.

6. Wait, Avelsman, Lorn, Introduction to Operational Amplifiers Theory and Applications, McGraw-Hill, New York, 1975.

7. P. Peebles, Communication System Principles, Addison-Westey, Reading, Mass., 1976.

8. J. F. Pierce, T. J. Paulus, Applied Electronics, Charles E. Merrill, Columbus, Ohio, 1972.

9. Stanford Goldman, Laplace Transform Theory and Electrical Transients, Doves, Inc., New York, 1976.

10. P. W. Nicholson, Nuclear Electronics, John Wiley & Sons, New York, 1974.

11. Advance Instrumentation for Reflood Studies (AIRS) Electronic System, Part A, AIRS 5, First Report, April 1979.

APPENDIXES

APPENDIX A

```
C
C
C       THIS PROGRAM COMPUTES THE FREQUENCY RESPONSE
C       OF THE LOOP TRANSMISSION FOR STABILITY ANALYSIS
C       WHERE THE COMPENSATION CAN BE VARIED TO OBSERVE
C       THE PHASE MARGIN AND CROSS-OVER FREQUENCY.
C
C
        REAL C1,C2,C3,R1,R2,R3,TMID,F,K,CP,FC,PM,PHASE
        REAL FZ1,FP1,FP2
        COMPLEX N1,D1,D2,D3,T
1       LAST=10000.00E3
        F=1.0
        C1=0.047E-6
        C2=56.0E-12
        R1=6.2E3
        R2=100.0E3
        R3=1.21E3
        TYPE 5
5       FORMAT (' DO YOU WANT TO CHANGE C3,Y=1,N=0')
        ACCEPT 10,W
10      FORMAT(I1)
        IF(W.EQ.0) GO TO 25
        TYPE 15
15      FORMAT(' ENTER VALUE OF C3 (FORMAT E11.4)')
        ACCEPT *,C3
25      TYPE 26
26      FORMAT(' DO YOU WANT TO CHANGE CP? (Y=1,N=0)')
        ACCEPT 10,W1
        IF(W1.EQ.0) GO TO 40
        TYPE 30
30      FORMAT(' ENTER VALUE OF CP (FORMAT E11.4)')
        ACCEPT *,CP
        TYPE 35
35      FORMAT(' ENTER OUTPUT VOLTAGE FOR CASE OF PROBE CAPACITANCE')
        ACCEPT *,VT
C
C
C       START LOOP GAIN COMPUTATIONS
C       STARTING BY COMPUTING POLE LOCATIONS
C
C
        FZ=0.159/(R3*C3)
        FP1=0.159/(C1*((R1*R2)/(R1+R2)))
        FP2=0.159*(C2+C3)/(R3*C2*C3)
40      AG=(2.048*33E-12)/(VT*CP*3.3)
        K=(CP/33E-12)*3.3*(1/(3.1416*383))*AG
        TMID=K*(R1*R2/(R1+R2))/(R2*(C2+C3)*2*3.1416)
        TMIDDB=20*ALOG10(TMID)
        N1=CMPLX(1.0,F/FZ)
        D1=CMPLX(0.0,F)
        D2=CMPLX(1.0,F/FP1)
        D3=CMPLX(1.0,F/FP2)
C
C
        T=TMID*N1/(D1*D2*D3)
C
C
        ABSVAL=CABS(T)
        PHASE=57.29578*ATAN2(AIMAG(T),REAL(T))
```

```
      PM=180+PHASE
      F=F*1.01
      IF(ABSVAL.LE.1.0) GO TO 50
      IF(F.LE.LAST) GO TO 40
      GO TO 999
C
C
C     OUTPUT RESULTS
C
C
50    TYPE 60,FZ,FP1,FP2
      PRINT 60,FZ,FP1,FP2
60    FORMAT(' POLE LOCATIONS: '/
     1 ' FZ= ',F10.3,2X,'FP1= ',F10.3,2X,'FP2= ',F12.3/)
      TYPE 70,R1,R2,R3,C1,C2,C3,CP,F,PM,PHASE,TMID,TMIDDB
      PRINT 70,R1,R2,R3,C1,C2,C3,CP,F,PM,PHASE,TMID,TMIDDB
70    FORMAT(' COMPONENT VALUES:'/
     1 ' R1= ',F10.3,6X,'R2= ',F10.3,7X,'R3= ',F10.3,/
     2 ' C1= ',E14.7,2X,'C2= ',E14.7,3X,'C3= ',E14.7,//
     3 ' PROBE CAPACITANCE: CP= ',E14.7,//
     4 ' FREQUENCEY FC= ',F10.4,5X,'PM= ',F7.3,5X,'PHASE= ',F10.3,//
     5 ' TMID= ',F12.4,3X,'TMID (DB)= ',F10.4//)
      PRINT 100,K
100   FORMAT(' K=',1X,E14.7/)
      PRINT 102,VT
102   FORMAT(' OUTPUT VOLTAGE FOR CP= ',F5.1/////)
      TYPE 800
800   FORMAT(' DO YOU WANT TO CONTINUE Y=0,N=1')
      ACCEPT 10,W2
      IF(W2.EQ.0) GO TO 1
999   STOP
      END
```

APPENDIX B

The model used for computer analysis (T) is shown in Fig. B.1. The nodes and branches are defined by circles and B# respectively.

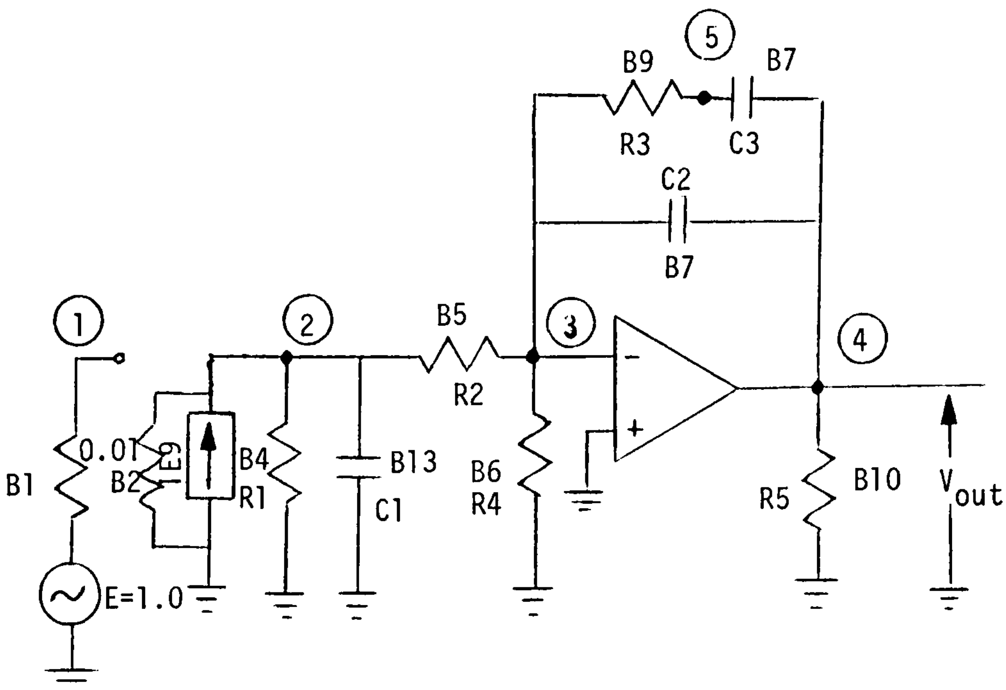

Figure B.1. Model for computing loop transmission

```
C
C
C        THIS PROGRAM COMPUTES THE LOOP TRANSMISSION
C        USING PCAP PROGRAM. THE BRANCHES AND NODES
C        ARE DEFINED IN THE MODEL.
C
C


//THESIS   JOB(44261,*****,REMOTE1,G-X),LUIS BRYAN
// EXEC PCAP
//GO.SYSIN DD *


AC ANALYSIS


B1       N(1,0),E=1.0,R=0.01
B2       N(2,0),R=1E9
B3       N(2,0),C=C1
B4       N(2,0),R=R1
B5       N(2,3),R=R2
B6       N(3,0),R=R4
B7       N(4,3),C=C2
B8       N(4,5),C=C3
B9       N(5,3),R=R3
B10      N(4,0),R=R5


C        A1 IS THE AMPLIFIER CARD FOR THE CONSTANT
C        CURRENT SOURCE DEFINED BY K AND VARIES
C        DEPENDING ON THE PROBE CAPACITANCE USED
C        FOR CALCULATING THE LOOP GAIN.


A1       B(1,10),GM=K
OA1      N(3,4,0)


C        OA1 IS THE OPERATIONAL AMPLIFIER CARD WHICH
C        USES THE LIBRARY MODEL OF PCAP


FREQ=1(*1.24)100E3
TAB,NV4
EXECUTE
MODIFY
CANCEL
FREQ=1(*1.24)100E3
PLOT,LG(1,4)
EXECUTE
END
```

APPENDIX C

The model used for computer analysis (A_{cl}) is shown in Fig. C.1. The nodes and branches are defined by circles and B# respectively.

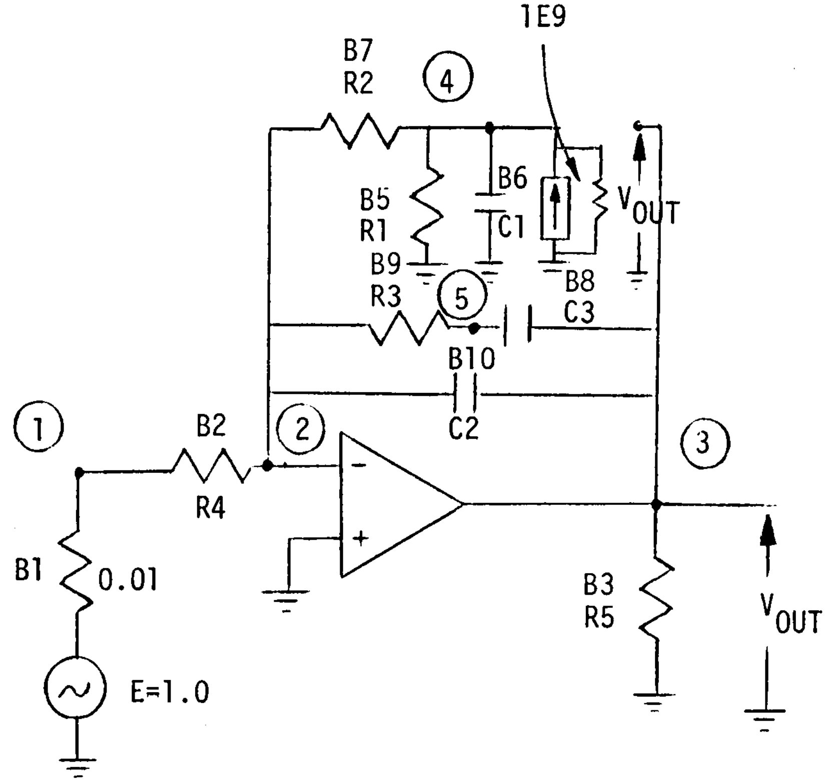

Figure C.1. Model for computing closed-loop frequency response.

```
C
C
C       THIS PROGRAM COMPUTES THE CLOSED LOOP RESPONSE
C       USING PCAP PROGRAM. THE BRANCHES AND NODES
C       ARE DEFINED IN THE MODEL.
C
C


//THESIS    JOB(44261,*****,REMOTE1,G-X),LUIS BRYAN
// EXEC PCAP
//GO.SYSIN DD *


        AC ANALYSIS


B1      N(1,0),E=1.0,R=0.01
B2      N(1,2),R=R4
B3      N(3,0),R=R5
B4      N(3,4),R=1E9
B5      N(4,0),R=R1
B6      N(4,0),R=C1
B7      N(4,2),R=R2
B8      N(3,5),C=C3
B9      N(5,2),R=R3
B10     N(3,2),C=C2


C       A1 IS THE AMPLIFIER CARD FOR THE CONSTANT
C       CURRENT SOURCE DEFINED BY K AND VARIES
C       DEPENDING ON THE PROBE CAPACITANCE USED
C       FOR CALCULATING THE LOOP GAIN.


A1      B(3,4),GM=K
OA1     N(2,3,0)


C       OA1 IS THE OPERATIONAL AMPLIFIER CARD WHICH
C       USES THE LIBRARY MODEL OF PCAP


        FREQ=1(*1.24)100E3
        TAB,NV3
        EXECUTE
        MODIFY
        CANCEL
        FREQ=1(*1.24)100E3
        PLOT,LG(1,3)
        EXECUTE
        END
```

APPENDIX D

The model used for computer analysis (transient) is shown in Fig. D.1. The nodes and branches are defined by circles and B# respectively.

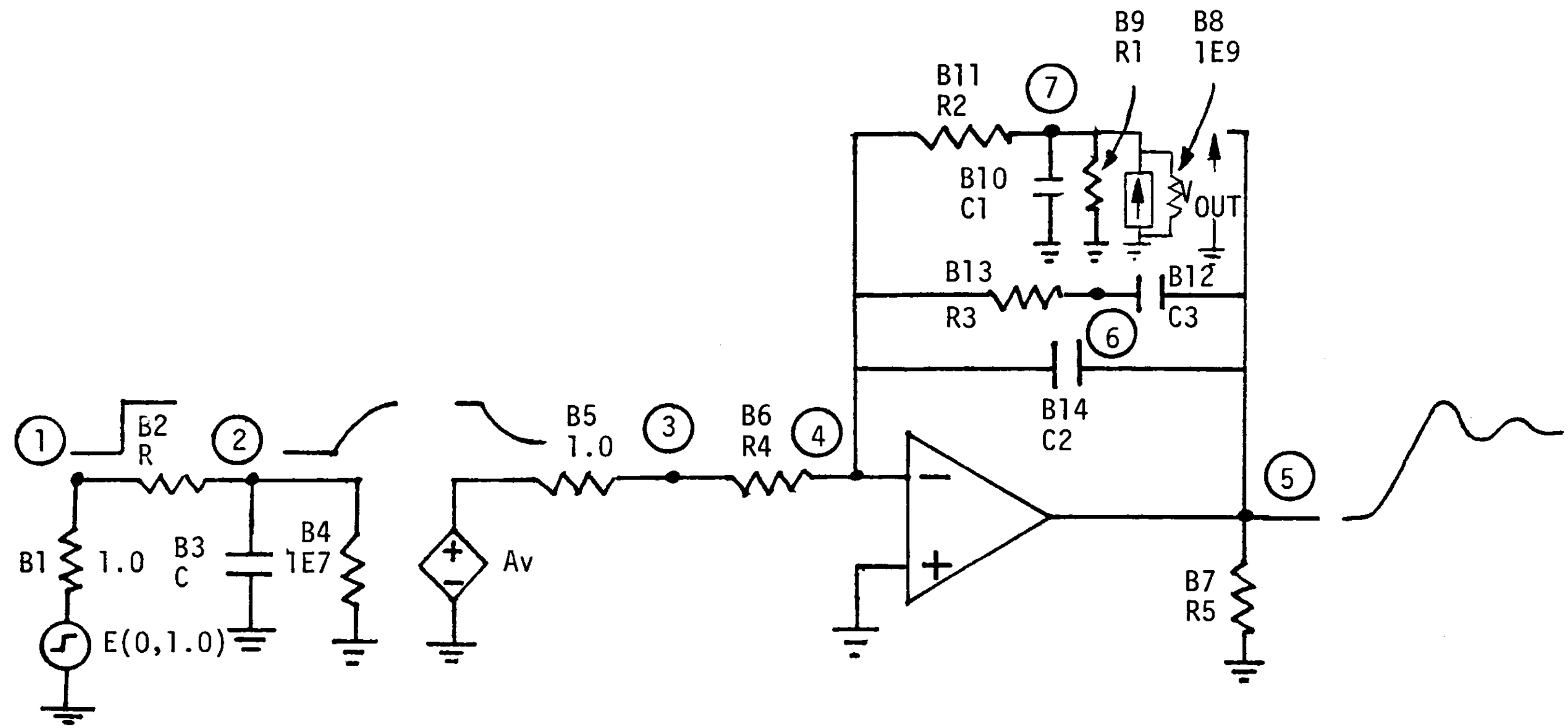

Figure D.1. Model for computing transient response

```
C
C        THIS PROGRAM COMPUTES THE TRANSIENT RESPONSE
C        USING PCAP PROGRAM. THE BRANCHES AND NODES
C        ARE DEFINED IN THE MODEL.
C

//THESIS    JOB(44261,*****,REMOTE1,G-X),LUIS BRYAN
// EXEC PCAP
//GO.SYSIN DD *

TRANSIENT


B1       N(1,0),R=1.0
B2       N(1,2),R=R
B3       N(2,0),C=C
B4       N(2,0),R=1E7
B5       N(3,0),R=1.0
B6       N(3,4),R=R4
B7       N(5,0),R=R5
B8       N(5,7),R=1E9
B9       N(7,0),R=R1
B10      N(7,0),C=C1
B11      N(7,4),R=R2
B12      N(5,6),C=C3
B13      N(6,4),R=R3
B14      N(5,4),C=C2


C        A1 IS THE DEPENDENT VOLTAGE SOURCE USED
C        TO INVER THE INPUT   VSET.
C        A2 IS THE DEPENDENT CURRENT SOURCE WHICH IS
C        VARIED DEPENDING ON THE PROBE CAPACITANCE. ITS
C        VALUE IS DEFINED BY K.
C        OA1 IS THE OPERATIONAL AMPLIFIER CARD WHICH USES
C        THE PCAP LIBRARY MODEL.
C        E1 IS THE   VSET CARD USED FOR THE TRANSIENT
C        RESPONSE.


A1       B(4,5),VG=1.0
A2       B(7,8),GM=K
OA1      N(4,5,0)


E1       A1(1E-9),0,   VSET
         TIME STEP=1.8E-6
         OUTPUT INTERVAL=20
         FINAL TIME=1.8E-3
         PLOT,NV(2),NV(3),NV(5)
         EXECUTE
         END
```

VITA

Luis Arturo Bryan was born on May 24, 1956 in Panama, Republic of Panama. He attended primary and secondary education at Colegio La Salle in Panama, where he graduated in December 1973. Before entering The University of Tennessee, he attended Abraham Baldwin College and Shorter College. In March 1978, he received a Bachelor of Science degree in Electrical Engineering. During his senior year at The University of Tennessee he worked as a student research assistant. After accepting a research and teaching assistantship for a year, he began graduate studies. In April 1979, he accepted a consulting job with E. G. & G. Oak Ridge Operations related to his Master's thesis. He received a Master of Engineering degree in Electrical Engineering in December 1979.

The author is a member of Eta Kappa Nu, Phi Kappa Phi, and the Institute of Electrical and Electronic Engineers.